A mathematical model of the visual MacKay effect

Cyprien Tamekue, Dario Prandi, Yacine Chitour

A MATHEMATICAL MODEL OF THE VISUAL MACKAY EFFECT

CYPRIEN TAMEKUE, DARIO PRANDI, AND YACINE CHITOUR

Abstract. This paper investigates the intricate connection between visual perception and the mathematical modeling of neural activity in the primary visual cortex (V1). The focus is on modeling the visual MacKay effect [D. M. MacKay, Nature, 180 (1957), pp. 849–850]. While bifurcation theory has been a prominent mathematical approach for addressing issues in neuroscience, especially in describing spontaneous pattern formations in V1 due to parameter changes, it faces challenges in scenarios with localized sensory inputs. This is evident, for instance, in Mackay's psychophysical experiments, where the redundancy of visual stimuli information results in irregular shapes, making bifurcation theory and multi-scale analysis less effective. To address this, we follow a mathematical viewpoint based on the input-output controllability of an Amari-type neural fields model. In this framework, we consider sensory input as a control function, a cortical representation via the retino-cortical map of the visual stimulus that captures its distinct features. This includes highly localized information in the center of MacKay's funnel pattern "MacKay rays". From a control theory point of view, the Amari-type equation's exact controllability property is discussed for linear and nonlinear response functions. For the visual MacKay effect modeling, we adjust the parameter representing intra-neuron connectivity to ensure that cortical activity exponentially stabilizes to the stationary state in the absence of sensory input. Then, we perform quantitative and qualitative studies to demonstrate that they capture all the essential features of the induced after-image reported by MacKay.

Keywords. Control in neuroscience, Exact controllability, Neural field model, Amari-type equation, Visual illusions and perception, MacKay effect, Spatially forced pattern forming system.

MSCcodes. 93C20, 92C20, 35B36, 45A05, 45K05.

Contents

This work was supported by ANR-20-CE48-0003 and ANR-11-IDEX-0003, Objet interdisciplinaire H-Code. The work of the first author was supported by a grant from the bourse de thèses "Jean-Pierre Aguilar".

1. Introduction

A simple yet profound question that can arise in humans daily is how we can control the complexities around us, whether they are mathematical equations or even our perceptions of reality. With its intricate network of neurons, the brain is a prime example of a complex system that can be understood through the lens of control theory. Neuroscientists and psychophysics researchers have been fascinated by intriguing phenomena like the MacKay effect [17, 18] during which people experience visual illusions. In contrast to a visual hallucination, which refers to the perception of an image that does not exist or is not present in front of the person who has experienced it, a visual illusion often occurs when external stimuli trick our brain into perceiving something differently from its actual state.

In the last decades, investigations of mechanisms underlying the spontaneous perception of visual hallucination patterns have been widely undertaken in the literature using neural dynamics in the primary visual cortex (hereafter referred to as V1) when its activity is due solely to the random firing of its spiking neurons, that is in the absence of sensory inputs from the retina, [4, 8, 12, 28, 5]. In their seminal work [8], by using bifurcation techniques near a Turing-like instability, Ermentrout and Cowan found that the 2-dimensional two-layer neural fields equation modelling the average membrane potential of spiking neurons in V1 derived by Wilson and Cowan in [32] is sufficient to theoretically describe the spontaneous formation (i.e., in the absence of visual sensory inputs) of some geometric patterns (horizontal, vertical and oblique stripes, square, hexagonal and rectangular patterns, etc.) in V1. These patterns result from activity spreading over this brain area and correspond to states of highest cortical activities. When we transform these patterns by the inverse of the retino-cortical map from V1 onto the visual field [29, 22], what we obtain in the retina in terms of images are geometric visual hallucinations. They correspond to some of the form constants that Klüver had meticulously classified [15], mainly those contrasting regions of white and black (funnel, tunnel, spiral, checkerboard, phosphenes). Therefore, the neural dynamic equation used to model the cortical activity in V1 combined with the bijective nonlinear retino-cortical mapping between the visual field and V1 predicts the geometric forms of hallucinatory patterns.

While spontaneous patterns that emerge in V1 give us insight into the underlying architecture of the brain's neural network, little is known about how precisely the intrinsic circuitry of the primary visual cortex generates the patterns of activity that underlie the visual illusions induced by visual stimuli from the retina. We study in this paper the interaction between retinal stimulation by geometrical patterns and the cortical response in the primary visual cortex, focusing on the MacKay effect [17] replication using control of Amari-type equation. As a control term, we consider the sensory input from the retina modelling the V1 representation via the retino-cortical map of the visual stimulus used in this intriguing visual phenomenon.

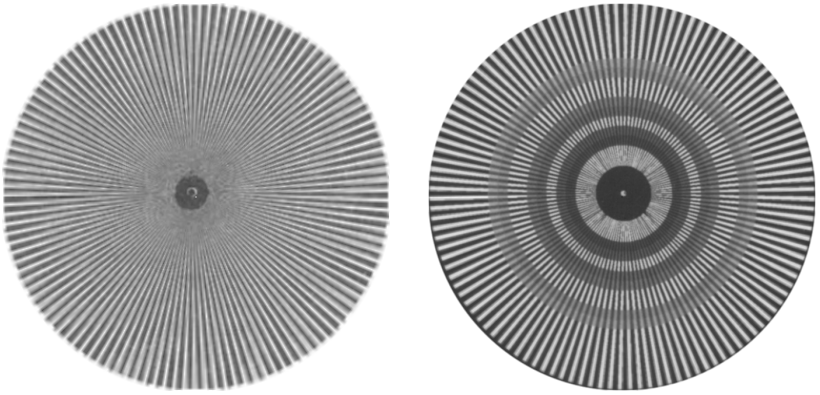

FIGURE 1. The MacKay effect [17], showcasing the illusion induced by the stimulus on the left, referred to as "MacKay rays". This stimulus leads to an illusory perception of concentric rings superimposed in its background, as illustrated on the right. To see the illusory contours, look at the centre of the black circle in the image on the *left*. The adaptation of this figure is based on the original representation from [17, Fig. 1] and [33, Fig. 1b].

1.1. **The visual MacKay effect.** Around 1960, Donald MacKay made notable observations on the after-effects of visual stimulation using regular geometrical patterns containing highly redundant information. He associated this phenomenon, now known as the "MacKay effect", with a specific region of the visual cortex that potentially benefits from such redundancy [17]. The psychophysical experiments presented in this paper demonstrate that when a highly redundant visual stimulus, such as a funnel pattern (fan shapes), is presented at the center of the stimulus, an accompanying illusory tunnel pattern (concentric rings) emerges in the visual field, superimposed onto the stimulus pattern (see Fig. 1).

Notably, the distance from the pattern to the retina or the illumination does not significantly affect these more intricate phenomena. For most observers, the illusory contours in the background of the afterimage rotate rapidly at right angles to the stimulus pattern, either clockwise or counterclockwise. Similarly, many observers perceive an illusory funnel pattern superimposed in the afterimage background when viewing a tunnel pattern as that of Figure 2, the right panel. In both cases, observers often note rapidly fluctuating sectors, again rotating either clockwise or counterclockwise. Notably, the stimulus pattern does not need to fill the entire visual field; a portion of the stimulus is sufficient to generate a corresponding afterimage in the same portion. However, in both cases, the nervous system tends to prefer the direction perpendicular to the regular contours of the visual stimulus. The present paper proposes to attribute this preference to the retino-cortical map, resulting in induced afterimages of superimposed patterns of horizontal and vertical stripes in V1.

1.2. **Strategy of study and presentation of our results.** In Section 1.2.1, we expound on our strategy to theoretically replicate the visual MacKay effect that we recalled in the previous section. Subsequently, in Section 1.2.2, we present and discuss our findings.

This work originated in [27], where we developed a novel approach to describe the MacKay effect specifically, associated with a funnel pattern containing high localized information in the center of the image (*created by the very fast alternation of black and white rays*) [17]. Instead of relying on traditional mathematical tools such as bifurcation analysis, perturbation theories,

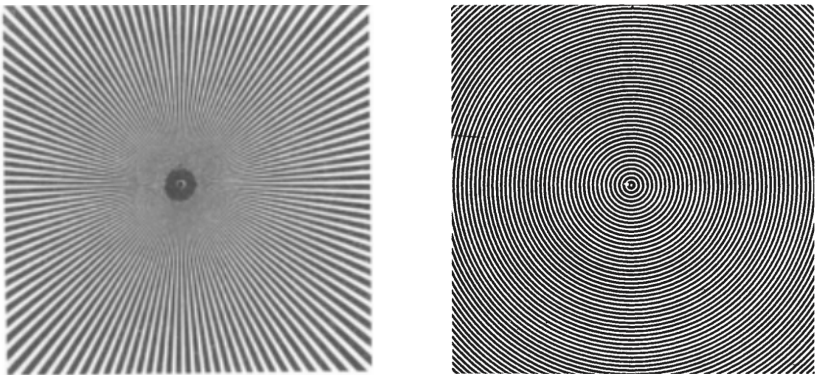

FIGURE 2. The stimuli used in [17]. *Left:* "MacKay-rays". *Right:* "MacKay-target".

or multi-scale analysis, commonly used to address neuroscience questions, we sought alternative methods via control of the Amari-type neural fields.

Indeed, these classical mathematical tools are highly suitable for describing phenomena like spontaneous geometric visual hallucinations that emerge in the visual field due to sudden qualitative changes in specific physiological parameters [4, 8, 12, 28]. They also prove effective in understanding sensory-driven and self-organized cortical activity interactions when the visual stimulus exhibits regular shape and complete distribution across the visual field, with symmetry respecting a subgroup of the Euclidean group [19]. In simple terms, these tools are appropriate when dealing with equations that exhibit complete equivariance (commutation) with respect to a given group, typically the Euclidean group. However, the original MacKay stimulus, known as the "MacKay rays" (refer to Fig. 2), consists of funnel patterns with high localized information in the center. As a result, the Euclidean symmetry of the V1 representation via the retino-cortical map of the funnel patterns is broken (see Section 2.2). This corresponds to the fact that the funnel pattern is invariant by dilations in the visual plane, while the "MacKay rays" are not. As a consequence, the Amari-type neural field describing the V1 activity induced by "MacKay rays" does not present any symmetry. Accordingly, neither the works of [4, 8] nor [19] can be directly employed to describe these complex visual phenomena. In particular, the work [19] theoretically replicate a variant of the MacKay effect where the visual stimulus is not the "MacKay rays" nor the "MacKay target" (see Figure 2, right) but a regular (symmetric with respect to some subgroups of the plane Euclidean group) funnel or tunnel patterns, which is fully distributed in the visual field.

1.2.1. *Strategy of study.* In our study, we begin by assuming that neurons in V1 are interconnected in a homogeneous and isotropic manner. Accordingly, we employ the following Amari-type equation [1, Eq. (3)] to describe the average membrane potential of V1 spiking neurons that take into account the sensory input from the retina:

$$\partial_t a = -a + \mu\omega * f(a) + I. \tag{NF}$$

Here $a : \mathbb{R}_+ \times \mathbb{R}^2 \to \mathbb{R}$ is a function of time $t \in \mathbb{R}_+$ and the position $x \in \mathbb{R}^2$, the sensory input I represents the projection of the visual stimulus into V1 by the retino-cortical map. The connectivity kernel $\omega(x, y) = \omega(|x - y|)$ models the strength of connections between neurons located at positions $x \in \mathbb{R}^2$ and $y \in \mathbb{R}^2$. The function f captures the nonlinear response of

neurons after activation, while the parameter $\mu > 0$ characterizes the intra-neural connectivity. The symbol $*$ denotes spatial convolution, as defined in (3) below.

We observe that it would be natural to model V1 as a bounded domain Ω, instead of $\mathbb{R}^2$. We stress that due to the strongly localized connectivity kernel that we consider, our results could in principle be extended to this case, at least to describe neuronal activity sufficiently far from the boundary of Ω. Moreover, although the more plausible biological neuronal dynamics in V1 involve considering the orientation preferences of "simple cells" as done in [4, Eq. (1)] when describing contoured spontaneous cortical patterns, we neglect the orientation label entirely and focus on equation (NF). This simplification is motivated by the fact that equation (NF) is sufficient for describing spontaneous funnel and tunnel patterns, and we expect it also to be suitable for describing psychophysical experiments involving these patterns.

In psychophysical experiments, observers perceive an illusory afterimage in their visual field when viewing the visual stimulus, and this afterimage persists for a few seconds. Therefore, describing these intriguing visual phenomena in V1 using equation (NF) relies on explicitly studying the map Ψ, which associates the sensory input I with its corresponding stationary output $\Psi(I)$. The stationary output represents the stationary solution of equation (NF) for a given I. Our goal is to prove that the cortical activity $a(t, \cdot)$, which is the solution of equation (NF), exponentially stabilizes towards $\Psi(I)$ as $t \to +\infty$. Then, we perform qualitative and quantitative study of this stationary state in a convenient space.

Before performing the asymptotic study (qualitatively and quantitatively) of the input to stationary output map for modelling the visual MacKay effect, we investigate the exact controllability properties of the Amari-type control system (NF) where we interpret the sensory input I as a distributed control over $\mathbb{R}^2$ that we use to act on the system state modelled by the cortical activity a. In that direction, we prove that (NF) is exactly controllable, in the sense explained previously, except for certain particular functional frameworks.

1.2.2. *Presentation of results.* In our previous paper [27], we established that to accurately model the visual stimuli used, for instance, in the MacKay effect associated with the "MacKay rays" visual stimulus, it is crucial to consider the highly localized information present in the center of the funnel patterns as created by the very fast alternation of black and white rays. This observation arises from the underlying Euclidean symmetry of V1, which imposes restrictions on the geometric shapes of sensory inputs capable of inducing cortical illusions in V1. Interestingly, this mathematical evidence supports the observation previously made by MacKay in paragraph 2 of [17]: *"[$\cdots$] in investigations of the visual information system, it might be especially interesting to observe the effect of highly redundant information patterns since the nervous system might conceivably have its own ways of profiting from such redundancy [$\cdots$]"*.

To model the redundant information in the center of the funnel pattern created by the very fast alternation of black and white rays, we employed the characteristic function of a small disk in the center of the visual field as a control function. Through numerical simulations, we suggested that equation (NF), together with an *odd* sigmoidal response function, successfully reproduces the MacKay effect associated with the "MacKay rays". We employed a similar approach to reproduce the MacKay effect associated with the "MacKay target", except that the control function was chosen as the characteristic function of two symmetric rays converging towards the center of the image (refer to Remark 5.13 for more details on this modelling).

Having established that equation (NF), with appropriate modelling of MacKay visual stimuli, reproduces this phenomenon, our next objective was to provide a mathematical proof of the numerical results obtained in [27]. Therefore, in [26], we discovered that the linearized version

of (NF) is sufficient to describe and replicate the MacKay effect, indicating that the nonlinear nature of the response function does not play a role in its reproduction. Specifically, the saturation effect only serves to dampen high oscillations that can occur in V1.

In this paper, we provide a mathematical modelling of the visual MacKay effect using Equation (NF), employing complex and harmonic analysis tools and sharp inequality estimates. Specifically, we exploit Fourier analysis.

To the authors' knowledge, the only attempt to theoretically replicate the MacKay-like phenomenon using neural fields equations has been undertaken by Nicks *et al.* [19]. They employed a model of cortical activity in V1, which included spike-frequency adaptation (SFA) of excitatory neurons, and utilized bifurcation and multi-scale analysis near a Turing-like instability to describe the MacKay-type effect associated with a fully distributed state-dependent sensory input representing cortical representations of funnel and tunnel patterns. By assuming a balanced condition[1] on the interaction kernel, they derived a dynamical equation for the amplitude of the stationary solution near the critical value μ_c (see Equation (1) below) of the parameter μ where spontaneous cortical patterns emerge in V1. Their theoretical results do not apply to localized inputs, as those employed by MacKay [17].

In the present study, to address the specificity of the sensory inputs utilized in these psychophysical experiments (i.e., the highly localized information in MacKay's stimuli), we rely on a central assumption regarding the range of parameter μ. We assume that μ is smaller than the threshold μ_c, given as follows,

$$\mu_c := \frac{1}{f'(0)\max\limits_{\xi\in\mathbb{R}^2}\hat{\omega}(\xi)}, \tag{1}$$

corresponding to the value of μ where cortical patterns spontaneously emerge in V1, [8, 4].

Finally, we stress once again that our focus lies in assessing the qualitative concordance between the outputs of the proposed models and the observed human perceptual response to these illusions reported by MacKay. It is imperative to emphasize that this inquiry is qualitative, demonstrating the potential utility of Amari-type dynamics in reproducing the perceptual distortions elicited by certain visual illusions.

1.3. **Structure of the paper.** The remaining of the paper is organized as follows: Section 1.4 begins by introducing the general notations that will be utilized throughout the paper. We present assumptions on model parameters used in Equation (NF) in Section 2.1, and we define a binary pattern necessary to represent cortical activity in terms of white and black zones in Section 2.2. In Section 3, we recall some preliminary results about the well-posedness of equation (NF), and in Section 4, we discuss the exact controllability properties of Equation (NF). Using equation (NF), in Section 5, we investigate the theoretical replication of the visual MacKay effect. In Section 5.4, we present numerical results to bolster our theoretical study. Finally, we provide in the Appendix some technical Theorems that serve as complement results.

1.4. **General notations.** Unless otherwise stated, p will denote a real number satisfying $1 \leq p \leq \infty$, and q will denote the conjugate to p given by $1/p + 1/q = 1$. We adopt the convention that the conjugate of $p = 1$ is $q = \infty$ and vice-versa.

For $d \in \{1, 2\}$, we denote by $L^p(\mathbb{R}^d)$ the Lebesgue space of class of real-valued measurable functions u on $\mathbb{R}^d$ such that $|u|$ is integrable over $\mathbb{R}^d$ if $p < \infty$, and $|u|$ is essentially bounded

[1] A kernel ω of "Mexican-hat" type distribution satisfies the balanced condition (between excitatory and inhibitory neurons) if its Fourier transform at zero equals 0.

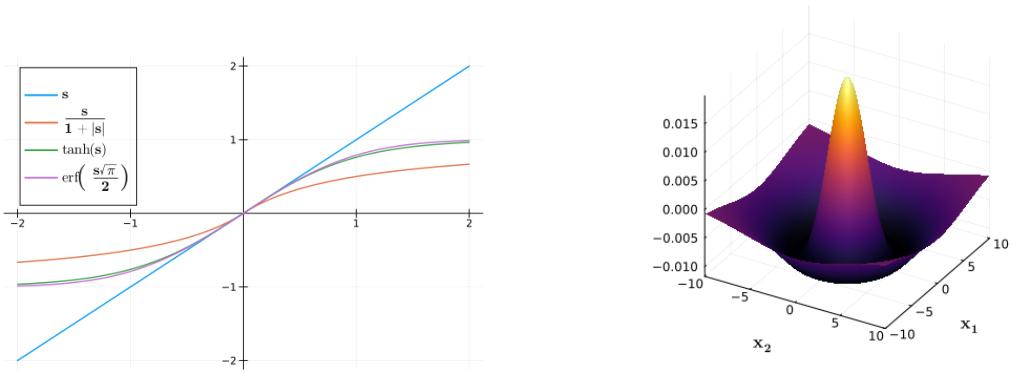

FIGURE 3. Possible response functions on the *left* where erf is the Gauss error function, and on the *right* a 2D DoG kernel ω. Here, $\kappa = 2$, $\sigma_1 = 2$, and $\sigma_2 = 4$.

over $\mathbb{R}^d$ when $p = \infty$. We endow these spaces with their standard norms

$$\|u\|_p^p = \int_{\mathbb{R}^d} |u(x)|^p dx, \qquad \text{and} \qquad \|u\|_\infty = \operatorname*{ess\,sup}_{x\in\mathbb{R}^d} |u(x)|.$$

We let $X_p := C([0,\infty); L^p(\mathbb{R}^d))$ be the space of all real-valued functions u on $\mathbb{R}^d \times [0,\infty)$ such that, $u(x,\cdot)$ is continuous on $[0,\infty)$ for a.e., $x \in \mathbb{R}^d$ and $u(\cdot,t) \in L^p(\mathbb{R}^d)$ for every $t \in [0,\infty)$. In X_p, we will use the following norm $\|u\|_{L_t^\infty L_x^p} = \sup_{t\geq 0} \|u(\cdot,t)\|_p$.

For $x \in \mathbb{R}^2$, we denote by $|x|$ its Euclidean norm, and the scalar product with $\xi \in \mathbb{R}^2$ is defined by $\langle x, \xi\rangle = x_1\xi_1 + x_2\xi_2$.

We let $\mathcal{S}(\mathbb{R}^d)$ be the Schwartz space of rapidly-decreasing $C^\infty(\mathbb{R}^d)$ functions, and $\mathcal{S}'(\mathbb{R}^d)$ be its dual space, i.e., the space of tempered distributions. Then, $\mathcal{S}(\mathbb{R}^d) \subset L^p(\mathbb{R}^d)$ and $L^p(\mathbb{R}^d) \subset \mathcal{S}'(\mathbb{R}^d)$ continuously. The Fourier transform of $u \in \mathcal{S}(\mathbb{R}^d)$ is defined by

$$\widehat{u}(\xi) := \mathcal{F}\{u\}(\xi) = \int_{\mathbb{R}^d} u(x) e^{-2\pi i \langle x,\xi\rangle} dx, \qquad \forall \xi \in \mathbb{R}^d. \tag{2}$$

We highlight that, for $1 \leq p \leq 2$, the above definition can be continuously extends to function $u \in L^p(\mathbb{R}^d)$ by density and Riesz-Thorin interpolation theorem. Whereas one can extend the above by duality to $\mathcal{S}'(\mathbb{R}^d)$. We recall that $\mathcal{F}$ is a linear isomorphism from $\mathcal{S}(\mathbb{R}^d)$ to itself and from $\mathcal{S}'(\mathbb{R})$ to itself.

The spatial convolution of two functions $u \in L^1(\mathbb{R}^d)$ and $v \in L^p(\mathbb{R}^d)$, $1 \leq p \leq \infty$ is defined by

$$(u * v)(x) = \int_{\mathbb{R}^d} u(x-y)v(y)dy, \qquad x \in \mathbb{R}^d. \tag{3}$$

Finally, the following notation will be helpful: if F is a real-valued function defined on $\mathbb{R}^2$, we use $F^{-1}(\{0\})$ to denote the zero level-set of F.

2. Assumptions on parameters and binary representation of patterns

We present in this section assumptions on model parameters used in Equation (NF) and the definition of a binary pattern necessary to represent cortical activity in terms of white and black zones.

2.1. **Assumption on parameters for Amari-type equation.** We assume that the response function f belongs to the class $C^2(\mathbb{R})$, is non-decreasing, satisfies $f(0) = 0$, $f'(0) = \max_{s\in\mathbb{R}} f'(s)$, and f'' is also bounded so that f' is Lipschitz continuous. Please refer to Figure 3 (image on the left) for an example of a response function.

Unless otherwise stated, we consider f to be linear or a nonlinear and sigmoid function, such that $\|f\|_\infty = 1$, $f'(0) = 1$. This is without loss of generality since, as long as $f'(0) \neq 0$, we can always define a sigmoid function $\widetilde{f}(s) = f(\lambda s)/\|f\|_\infty$ with $\lambda = \|f\|_\infty/f'(0)$ and $s \in \mathbb{R}$.

The interaction kernel ω is chosen to be the following difference of Gaussians (DoG)

$$\omega(x) = [2\pi\sigma_1^2]^{-1} e^{-\frac{|x|^2}{2\sigma_1^2}} - \kappa[2\pi\sigma_2^2]^{-1} e^{-\frac{|x|^2}{2\sigma_2^2}}, \qquad x \in \mathbb{R}^2, \tag{4}$$

where $\kappa > 0$, $0 < \sigma_1 < \sigma_2$, and $\sigma_1\sqrt{\kappa} < \sigma_2$. It is worth noting that this choice of interaction kernel aligns with the framework employing Equation (NF) to generate spontaneous cortical patterns in V1.

In particular, ω is homogeneous and isotropic with respect to the spatial coordinates. It solely depends on the Euclidean distance between neurons and exhibits rotational symmetry. The first (positive) Gaussian in (4) describes short-range excitation interactions, while the second (negative) Gaussian represents long-range inhibition interactions between neurons in V1.

It is important to observe that $\omega(x) = \omega(|x|)$ and that ω belongs to the Schwartz space $\mathcal{S}(\mathbb{R}^2)$, implying that $\omega \in L^p(\mathbb{R}^2)$ for all real numbers $1 \leq p \leq \infty$. The Fourier transform of ω can be explicitly expressed as

$$\widehat{\omega}(\xi) = e^{-2\pi^2\sigma_1^2|\xi|^2} - \kappa e^{-2\pi^2\sigma_2^2|\xi|^2}, \qquad \forall \xi \in \mathbb{R}^2, \tag{5}$$

and $\widehat{\omega}$ reaches its maximum at every vector $\xi_c \in \mathbb{R}^2$ such that

$$|\xi_c| = q_c := \sqrt{\frac{\log\left(\frac{\kappa\sigma_2^2}{\sigma_1^2}\right)}{2\pi^2(\sigma_2^2 - \sigma_1^2)}} \qquad \text{and} \qquad \max_{r\geq 0} \widehat{\omega}(r) = \widehat{\omega}(q_c). \tag{6}$$

Finally, the explicit expression for the L^1-norm of ω is given by

$$\|\omega\|_1 = (1-\kappa) + 2\left(\kappa e^{-\frac{\Theta^2}{2\sigma_2^2}} - e^{-\frac{\Theta^2}{2\sigma_1^2}}\right) \qquad \text{with} \qquad \Theta := \sigma_1\sigma_2\sqrt{\frac{2\log\left(\frac{\sigma_2^2}{\kappa\sigma_1^2}\right)}{\sigma_2^2 - \sigma_1^2}}. \tag{7}$$

We emphasize that the kernel ω does not necessarily satisfy the *balanced*[2] condition $\widehat{\omega}(0) = 0$ between excitation and inhibition. However, this condition is met when $\kappa = 1$.

2.2. **Binary representation of patterns.** Let us start this section by briefly recalling the retino-cortical map that can be found in [22, 4]. Let $(r, \theta) \in [0, \infty) \times [0, 2\pi)$ denote polar coordinates in the visual field (or in the retina) and $(x_1, x_2) \in \mathbb{R}^2$ Cartesian coordinates in V1. The retino-cortical map (see also [27] and references within) is analytically given by

$$re^{i\theta} \mapsto (x_1, x_2) := (\log r, \theta)\,. \tag{8}$$

[2]For a homogeneous NF equation (i.e., when $I = 0$), this condition ensures the existence of a unique stationary state $a_0 = 0$ even if $f(0) \neq 0$. It was assumed, for instance, in [19] for deriving the amplitude equation of the stationary state near the bifurcation point μ_c.

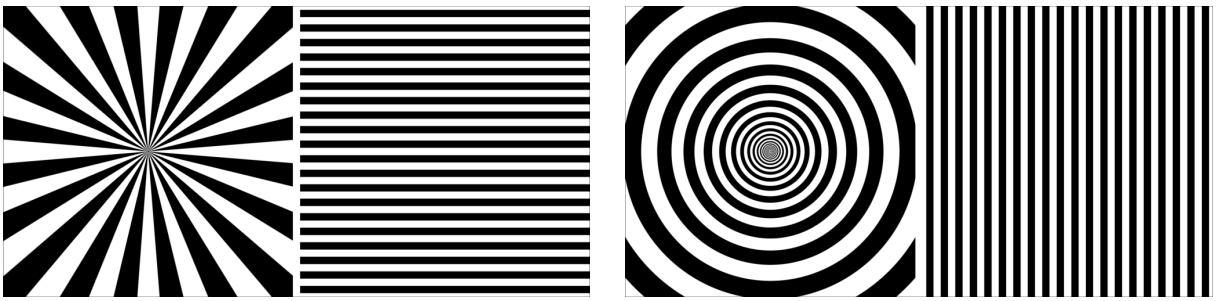

FIGURE 4. Funnel pattern on the *left* (respectively in the retina and V1). Tunnel pattern on the *right* (respectively in the retina and V1).

Due to the retino-cortical map (8), funnel and tunnel patterns are respectively given in Cartesian coordinates $x := (x_1, x_2) \in \mathbb{R}^2$ of V1 by

$$P_F(x) = \cos(2\pi\lambda x_2), \qquad P_T(x) = \cos(2\pi\lambda x_1), \quad \lambda > 0. \tag{9}$$

This choice is motivated by analogy with the (spontaneous) geometric hallucinatory patterns described in [8] and [4]. Given the above representation of funnel and tunnel patterns in cortical coordinates, to see how they look in terms of images, we represent them as contrasting white and black regions, see Figure. 4. More precisely, define the binary pattern B_h of a function $h : \mathbb{R}^2 \to \mathbb{R}$ by

$$B_h(x) = \begin{cases} 0, & \text{if } h(x) > 0 \quad \text{(black)} \\ 1, & \text{if } h(x) \leq 0 \quad \text{(white)}. \end{cases} \tag{10}$$

It follows that B_h is essentially determined by the zero level-set of h. Since stimuli involved in the MacKay effect are binary patterns, our strategy in describing these phenomena consists of characterising the zero-level set of output patterns. That is, we are mainly devoted to studying the qualitative properties of patterns by viewing them as binary patterns.

3. Well-posedness of the Cauchy problem and stationary state

We recall in this section some preliminary results about the well-posedness of equation (NF). We start this section by introducing the definition of stationary state to Equation (NF).

Definition 3.1 (Stationary state)**.** *Let $a_0 \in L^p(\mathbb{R}^2)$. For every $I \in L^p(\mathbb{R}^2)$, a stationary state $a_I \in L^p(\mathbb{R}^2)$ to Equation (NF) is a time-invariant solution, viz.*

$$a_I = \mu\omega * f(a_I) + I. \tag{SS}$$

Using standard assumptions on the kernel ω or on the response function f, it is straightforward to obtain the existence of at least one (even non-constant) stationary state to Equation (NF) when $I \equiv 0$, see for instance [4, 8, 19, 7]. Moreover, in the case of an inhomogeneous equation posed on a bounded domain with a state-dependent sensory input, in [6], under a mild condition on the boundness of the response function, the existence of at least one stationary state is proved using Schaefer's fixed point Theorem, see also [9]. However, in the face of an inhomogeneous equation posed on an unbounded domain as the case at hand, it can become a little bit more subtle to provide the existence of (non-constant) stationary state only with assumptions on ω and f.

Consistent with the strategy that we use in this work, in order to obtain a unique non-constant stationary state to the inhomogeneous Equation (NF), we will make the following assumption on the intra-neuron parameter $\mu > 0$,

$$\mu < \mu_0 := \|\omega\|_1^{-1}. \tag{11}$$

Observe that $\mu_0 \leq \mu_c$, where the latter is the bifurcation point defined in (1). We stress that, when $p = 2$, and under the balanced condition $\widehat{\omega}(0) = 0$, we can relax the above assumption to $\mu < \mu_c$, see Theorem 3.3.

We collect in the following lemma some useful estimates that are immediate consequences of generalised Young-convolution inequality.

Lemma 3.2. *Let $1 \leq p \leq \infty$. The nonlinear operator $X_p \ni a \mapsto \omega * f(a) \in X_p$ is well-defined and Lipschitz continuous and*

$$\|\omega * f(a) - \omega * f(b)\|_{L^p_x L^\infty_t} \leq \|\omega\|_1 \|a - b\|_{L^p_x L^\infty_t}, \qquad \forall a, b \in X_p. \tag{12}$$

Moreover,

(1) *If $a \in X_p$, then $\omega * f(a) \in X_\infty$ and*

$$\|\omega * f(a)\|_{L^\infty_x L^\infty_t} \leq \|\omega\|_q \|a\|_{L^p_x L^\infty_t}, \tag{13}$$

$$\|\omega * f(a)\|_{L^\infty_x L^\infty_t} \leq \|\omega\|_1; \tag{14}$$

(2) *If $a \in X_1$, then $\omega * f(a) \in X_p$,*

$$\|\omega * f(a)\|_{L^p_x L^\infty_t} \leq \|\omega\|_p \|a\|_{L^1_x L^\infty_t}. \tag{15}$$

In the following theorem, we prove the existence of a unique solution and a unique stationary state of the Cauchy problem associated with Equation (NF).

Theorem 3.3. *Let $1 \leq p \leq \infty$ and $I \in L^p(\mathbb{R}^2)$. For any initial datum $a_0 \in L^p(\mathbb{R}^2)$, there exists a unique $a \in X_p$, solution of Equation (NF). Moreover, there exists a unique stationary state $a_I \in L^p(\mathbb{R}^2)$ to (NF) under the following assumptions:*

i. *If $\mu < \mu_0$, then*

$$\|a(\cdot, t) - a_I(\cdot)\|_p \leq e^{-(1-\mu\|\omega\|_1)t} \|a_0(\cdot) - a_I(\cdot)\|_p, \qquad \text{for any } t \geq 0. \tag{16}$$

ii. *If $p = 2$, $\mu < \mu_c$, and $\hat{\omega}(0) = 0$, then*

$$\|a(\cdot, t) - a_I(\cdot)\|_2 \leq e^{-(1-\mu\|\widehat{\omega}\|_\infty)t} \|a_0(\cdot) - a_I(\cdot)\|_2, \qquad \text{for any } t \geq 0. \tag{17}$$

Proof. Equation (NF) can be seen as an ordinary differential equation in X_p, whose r.h.s. is a (globally) Lipschitz continuous map from X_p to itself by Lemma 3.2. It is then standard to obtain that for any initial datum $a_0 \in L^p(\mathbb{R}^2)$, Equation (NF) has a unique solution $a \in X_p$ (see, for instance, [30, 23]). Moreover, the map $\Phi_I : L^p(\mathbb{R}^2) \to L^p(\mathbb{R}^2)$ defined for all $u \in L^p(\mathbb{R}^2)$ by $\Phi_I(u) = I + \mu\omega * f(u)$ satisfies

$$\|\Phi_I(v) - \Phi_I(u)\|_p \leq \frac{\mu}{\mu_0} \|v - u\|_p, \qquad \forall u, v \in L^p(\mathbb{R}^2),$$

due to inequality (12). Since $\mu < \mu_0$, the existence of a unique stationary state $a_I \in L^p(\mathbb{R}^2)$ is obtained by invoking the contraction mapping principle.

We now present an argument of proof for Item *i.* of the statement. Set

$$b(x, t) = a(x, t) - a_I(x), \qquad (x, t) \in \mathbb{R}^2 \times [0, \infty), \tag{18}$$

It follows that b is the solution of the following initial value Cauchy problem

(19)
$$\begin{cases} \partial_t b(x,t) = -b(x,t) + \mu \displaystyle\int_{\mathbb{R}^2} \omega(x-y)[f(b(y,t)+a_I(y)) - f(a_I(y))]dy, & (x,t) \in \mathbb{R}^2 \times [0,\infty), \\ b(x,0) = a_0(x) - a_I(x), & x \in \mathbb{R}^2, \end{cases}$$

which belongs to $C([0,\infty); L^p(\mathbb{R}^2)) \cap C^1((0,\infty); L^p(\mathbb{R}^2))$. Moreover, b satisfies the following variations of constant formula

$$b(x,t) = e^{-t} b(x,0) + \mu \int_0^t e^{-(t-s)} \int_{\mathbb{R}^2} \omega(x-y)[f(b(y,t)+a_I(y)) - f(a_I(y))]dy, \tag{20}$$

for all $(x,t) \in \mathbb{R}^2 \times [0,\infty)$.

Taking the $L^p(\mathbb{R}^2)$-norm of the above identity, we find for every $t \geq 0$,

$$\|b(\cdot,t)\|_p \leq e^{-t}\|b(\cdot,0)\|_p + \mu\|\omega\|_1 \int_0^t e^{-(t-s)}\|b(\cdot,s)\|_p ds. \tag{21}$$

Applying Gronwall's Lemma to inequality (21) one deduces for every $t \geq 0$,

$$\|b(\cdot,t)\|_p \leq e^{-(1-\mu\|\omega\|_1)t}\|b(\cdot,0)\|_p.$$

This proves the inequality (16) and completes the proof of *i.*.

Let us now prove item *ii.* of the statement. In this case $p = 2$, $\mu < \mu_c$, and $\widehat{\omega}(0) = 0$. The latter condition implies that $\widehat{\omega}(|\xi|) \geq 0$ for all $\xi \in \mathbb{R}^2$. In particular, $\widehat{\omega}(q_c) = \max_{r\geq 0} \widehat{\omega}(r) = \|\widehat{\omega}\|_\infty$. Recall that $\Phi_I(u) = I + \mu\omega * f(u)$. Then, by Plancherel identity, the following holds for all $u, v \in L^2(\mathbb{R}^2)$,

$$\begin{aligned} \|\Phi_I(v) - \Phi_I(u)\|_2 = \|\widehat{\Phi_I(v)} - \widehat{\Phi_I(u)}\|_2 &= \mu\|\widehat{\omega}(\widehat{f(u)} - \widehat{f(v)})\|_2 \\ &\leq \mu\|\widehat{\omega}\|_\infty \|\widehat{f(u)} - \widehat{f(v)}\|_2 \\ &= \mu\widehat{\omega}(q_c)\|f(u) - f(v)\|_2 \\ &\leq \frac{\mu}{\mu_c}\|u - v\|_2. \end{aligned} \tag{22}$$

Here, the last inequality follows from $\mu_c = \hat{\omega}(q_c)^{-1}$ and the fact that f is 1-Lipschitz. Since $\mu < \mu_c$, the existence of a unique stationary state $a_I \in L^2(\mathbb{R}^2)$ is obtained by invoking the contraction mapping principle. We complete the proof by arguing as in the previous point and replacing (21) by

$$\|b(\cdot,t)\|_2 \leq e^{-t}\|b(\cdot,0)\|_2 + \mu\|\hat{\omega}\|_\infty \int_0^t e^{-(t-s)}\|b(\cdot,s)\|_2 ds. \tag{23}$$

□

Due to Theorem 3.3, we can introduce the following.

Definition 3.4. *Let $1 \leq p \leq \infty$, the nonlinear input-output map $\Psi : L^p(\mathbb{R}^2) \to L^p(\mathbb{R}^2)$ is defined by*

$$\Psi(I) = I + \mu\omega * f(\Psi(I)), \qquad \text{for all } I \in L^2(\mathbb{R}^2). \tag{24}$$

Proposition 3.5. *Let $1 \leq p \leq \infty$ and assume that $\mu < \mu_0$. Then,*

(1) *The map Ψ is well-defined, bi-Lipschitz continuous, and it holds*

$$\|\Psi(I)\|_p \leq \frac{\mu_0}{\mu_0 - \mu}\|I\|_p, \qquad \text{for all} \qquad I \in L^p(\mathbb{R}^2); \tag{25}$$

(2) *If $1 < p \leq \infty$, the map Ψ belongs to $C^1(L^p(\mathbb{R}^2); L^p(\mathbb{R}^2))$.*

Proof. We only provide the proof of item *1.*, for item *2.* see Theorem B.7. Let $I_1, I_2 \in L^p(\mathbb{R}^2)$. Then using inequality (12), we obtain

$$\|\Psi(I_1) - \Psi(I_2)\|_p \leq \frac{\mu}{\mu_0}\|\Psi(I_1) - \Psi(I_2)\|_p + \|I_1 - I_2\|_p.$$

It follows that

$$\|\Psi(I_1) - \Psi(I_2)\|_p \leq \frac{\mu_0}{\mu_0 - \mu}\|I_1 - I_2\|_p,$$

provided $\mu < \mu_0$. This implies that Ψ is Lipschitz continuous from $L^p(\mathbb{R}^2)$ to itself. On the other hand, thanks to inequality (12),

$$\begin{aligned} \|\Psi(I_1) - \Psi(I_2)\|_p &\geq \left| \|I_1 - I_2\|_p - \mu\|\omega * [f(\Psi(I_1)) - f(\Psi(I_2))]\,\|_p \right| \\ &\geq \|I_1 - I_2\|_p - \frac{\mu}{\mu_0}\|\Psi(I_1) - \Psi(I_2)\|_p. \end{aligned} \tag{26}$$

It follows that

$$\|I_1 - I_2\|_p \leq \left(1 + \frac{\mu}{\mu_0}\right)\|\Psi(I_1) - \Psi(I_2)\|_p.$$

This shows that Ψ is bijective and Ψ^{-1} is Lipschitz continuous from $L^p(\mathbb{R}^2)$ to itself. □

4. Controllability issues of Amari-type equation

In the area of mathematical neuroscience, the research by Ermentrout and Cowan [8] is notable for its pioneering insights into the spontaneous emergence of patterns in V1 using neural fields equations of Wilson-Cowan [32]. Likewise, Nicks *et al.* [19] provided a comprehensive understanding of how V1 patterns (orthogonally) respond to specific stimuli that are regular in shape and fill all the visual field, particularly near the threshold value μ_c via bifurcation theory and multi-scale analysis. However, these studies do not directly address, for instance, the MacKay effect associated with a funnel pattern that contains highly localized information in the center [17] or even Billock and Tsou's experiments [3] since the visual stimuli used in these experiences are non-regular in shape or localized in the visual field.

Building on our discussion in Section 1.2.2, we claim that these intriguing visual patterns in V1 should manifest before the μ parameter reaches the threshold μ_c. Given this, we are interpreting the MacKay effect using a controllability framework, specifically in relation to the Amari-type equation (NF). In this context, the sensory input is not just passive data; it acts as a control, shaping and reflecting V1's interpretation of the visual stimulus in the experiment.

We consider in this section the following nonlinear Amari-type control system,

$$\begin{cases} \partial_t a(x,t) + a(x,t) - \mu \displaystyle\int_{\mathbb{R}^2} \omega(x-y) f(a(y,t))dy = I(x) & (x,t) \in \mathbb{R}^2 \times [0,T], \\ \\ a(x,0) = a_0(x), & x \in \mathbb{R}^2, \end{cases} \tag{27}$$

where the cortical activity a represents the state of the system, $a_0 \in L^p(\mathbb{R}^2)$ is the initial datum, the sensory input $I \in L^p(\mathbb{R}^2)$ is the control that we will use to act on the system state and the time horizon $T > 0$.

Definition 4.1 (Exact controllability)**.** *Let $1 \leq p \leq \infty$. We say that the nonlinear control system (27) is exactly controllable in $L^p(\mathbb{R}^2)$ in time $T > 0$ if, for any $a_0, a_T \in L^p(\mathbb{R}^2)$, there*

exists a control function $I \in L^p(\mathbb{R}^2)$ *such that the solution of* (27) *with* $a(\cdot,0) = a_0$ *satisfies* $a(\cdot,T) = a_T$.

To comprehend how the exact controllability of the nonlinear control system (27) could be handled, let us first investigate the exact controllability of the linear model that we write in a more abstract way (initial value Cauchy problem) as follows,

$$\dot{a}(t) = Aa(t) + I, \qquad a(0) = a_0, \qquad t \in [0,T], \tag{28}$$

where the operator A is given by

$$Au = -u + \mu\omega * u, \qquad \forall u \in L^p(\mathbb{R}^2). \tag{29}$$

Observe that for any $1 \leq p \leq \infty$, the operator A is a linear bounded operator from $L^p(\mathbb{R}^2)$ to itself.

Proposition 4.2. *Let* $1 \leq p \leq \infty$. *Then, there exists a positive time* $\tau_0 > 0$ *such that the control system* (28) *is exactly controllable in* $L^p(\mathbb{R}^2)$ *in any time* $\tau \in (0, \tau_0)$.

Proof. Fix $T > 0$ and let $a_0, a_1 \in L^p(\mathbb{R}^2)$. Since e^{tA} is a uniformly continuous semigroup of bounded linear operators on $L^p(\mathbb{R}^2)$ for any $t \geq 0$, one can write

$$e^{tA} = \mathrm{Id} + O(t), \qquad t \geq 0,$$

where $O(t)$ is a linear and bounded operator of $L^p(\mathbb{R}^2)$ satisfying $\|O(t)\| \leq t\|A\|e^{t\|A\|}$, see for instance, [21, Theorem 1.2.]. Therefore, for any $\tau \in (0,T]$ and $a_\tau \in L^p(\mathbb{R}^2)$, the solution of (28) at time τ satisfies

$$a(\tau) = e^{\tau A}a_0 + \int_0^\tau e^{(\tau-s)A} I ds = e^{\tau A}a_0 + \tau(\mathrm{Id} + O(\tau))I. \tag{30}$$

Letting τ small enough, $\mathrm{Id} + O(\tau)$ is invertible in $\mathscr{L}(L^p(\mathbb{R}^2))$ (the vector space of linear and bounded operators from $L^p(\mathbb{R}^2)$ into itself), and $I = \tau^{-1}(\mathrm{Id} + O(\tau))^{-1}(a_1 - e^{\tau A}a_0) \in L^p(\mathbb{R}^2)$ defines a control function that steers the solution of (28) from a_0 to a_1 in time τ. □

Remark 4.3. *Note that in the linear case, when* $\mu < \mu_0$, *the control function* $I \in L^p(\mathbb{R}^2)$ *that steers the solution from the initial state* $a_0 \in L^p(\mathbb{R}^2)$ *to the target state* $a_1 \in L^p(\mathbb{R}^2)$ *in any time* $T > 0$ *is given by*

$$I = \left(\mathrm{Id} - e^{TA}\right)^{-1} A(a_1 - e^{TA}a_0). \tag{31}$$

Indeed, one can prove that the linear operator $A \in \mathcal{L}(L^p(\mathbb{R}^2))$ *is dissipative when* $\mu < \mu_0$ *and therefore that*

$$\|e^{tA}\|_{\mathcal{L}(L^p(\mathbb{R}^2))} < 1, \qquad \forall t > 0. \tag{32}$$

Let us now discuss the exact controllability in $L^p(\mathbb{R}^2)$ of the nonlinear system (27) that we write in abstract way as

$$\dot{a}(t) = N(a(t)) + I, \qquad a(0) = a_0, \qquad t \in [0,T], \tag{33}$$

where for any $1 \leq p \leq \infty$, the nonlinear operator N is defined by

$$N(u) = -u + \mu\omega * f(u), \qquad u \in L^p(\mathbb{R}^2). \tag{34}$$

Then (33) defines an ordinary differential equation in $L^p(\mathbb{R}^2)$ associated with N. Recall from Lemma 3.2 that for every $1 \leq p \leq \infty$, the nonlinear operator N is (globally) Lipschitz continuous

from $L^p(\mathbb{R}^2)$ to itself. Therefore, one can define a nonlinear[3] semigroup of operators $\{U(t,\cdot)\}_{t\geq 0}$ in $L^p(\mathbb{R}^2)$ such that for any $a_0 \in L^p(\mathbb{R}^2)$, $a(t) := U(t,a_0)$ is the unique solution to (33) when $I \equiv 0$, namely

$$\frac{\partial U}{\partial t}(t,a_0) = N(U(t,a_0)), \qquad U(0,a_0) = a_0. \tag{35}$$

Theorem 4.4. *Let $1 < p \leq \infty$. Then, there exists a positive time $\tau_0 > 0$ such that the control system (33) is exactly controllable in $L^p(\mathbb{R}^2)$ in any time $\tau \in (0,\tau_0)$.*

Proof. First of all, by Lemma B.8 one has $N \in C^1(L^p(\mathbb{R}^2); L^p(\mathbb{R}^2))$ and the Fréchet differential $DN(u) \in \mathscr{L}(L^p(\mathbb{R}^2))$ is uniformly bounded for every $u \in L^p(\mathbb{R}^2)$. Let $T > 0$ and $\tau \in (0,T]$.

By Lemma B.10, the differential of U with respect to a_0 is a well-defined invertible operator $D_{a_0}(t,v) \in \mathscr{L}(L^p(\mathbb{R}^2))$ for any $v \in L^p(\mathbb{R}^2)$ and every $0 < t \leq T$, and it satisfies

$$\|D_{a_0}U(t,v) - \mathrm{Id}\,\|_{\mathscr{L}(L^p(\mathbb{R}^2))} \leq t\left(1 + \frac{\mu}{\mu_0}\right) e^{\left(1+\frac{\mu}{\mu_0}\right)t}, \qquad 0 \leq t \leq T. \tag{36}$$

On the other hand, one observes that for any $a_0 \in L^p(\mathbb{R}^2)$ and every $I \in L^p(\mathbb{R}^2)$, the solution $a \in C([0,\tau]; L^p(\mathbb{R}^2))$ of (33) can be represented as

$$a(t) = U(t, g(t)), \qquad \text{where} \quad g(t) = a_0 + \int_0^t \mathcal{T}(s) I ds, \tag{37}$$

and we let $\mathcal{T}(s) := [D_{a_0}U(s,g(s))]^{-1}$. Again, by Lemma B.10, we have

$$\|\mathcal{T}(s) - \mathrm{Id}\,\|_{\mathscr{L}(L^p(\mathbb{R}^2))} \leq s\left(1 + \frac{\mu}{\mu_0}\right) e^{\left(1+\frac{\mu}{\mu_0}\right)s}, \qquad 0 \leq s \leq t. \tag{38}$$

Letting now $a_\tau \in L^p(\mathbb{R}^2)$, one can compute owing to (36) and (38),

$$\begin{aligned}
a_\tau := a(\tau) = U(\tau, g(\tau)) &= U(\tau,a_0) + \int_0^1 \frac{\partial}{\partial \eta} U\left(\tau, a_0 + \eta \int_0^\tau \mathcal{T}(s) I ds\right) d\eta \\
&= U(\tau,a_0) + \left\{\int_0^1 \left[D_{a_0}U\left(\tau, a_0 + \eta \int_0^\tau \mathcal{T}(s) I ds\right)\right]\left(\int_0^\tau \mathcal{T}(s) I ds\right) d\eta\right\} \\
&= U(\tau,a_0) + \left\{\int_0^1 (\mathrm{Id} + O(\tau)) \int_0^\tau (\mathrm{Id} + O(s)) ds d\eta\right\} I \\
&= U(\tau,a_0) + \tau(\mathrm{Id} + O(\tau)) I. \qquad (39)
\end{aligned}$$

Then, letting $\tau \in (0,T]$ small enough, one finds that $\mathrm{Id} + O(\tau)$ is invertible in $\mathscr{L}(L^p(\mathbb{R}^2))$ and $I = \tau^{-1}(\mathrm{Id} + O(\tau))^{-1}(a_\tau - U(\tau,a_0)) \in L^p(\mathbb{R}^2)$ defines a control function that steers the solution of (33) from a_0 to a_τ in time τ. □

Remark 4.5. *It is immediate to see that for large time $T > 0$, the control I_1 defined by $I_1 = 0$ on $[0, T-\tau]$ and $I_1 = \tau^{-1}(\mathrm{Id} + O(\tau))^{-1}(a_1 - e^{\tau A}a(T-\tau))$ on $(T-\tau, T]$ (resp. $I_2 = 0$ on $[0,T-\tau]$ and $I_2 = \tau^{-1}(\mathrm{Id} + O(\tau))^{-1}(a_1 - U(T, a(T-\tau)))$ on $(T-\tau,T]$) is a piece-wise constant function in $L^p(\mathbb{R}^2)$ that steers the solution of (28) (resp. (33)) from a_0 to a_1 in time T.*

Remark 4.6. *Related to Theorem 4.4 in the case of $p = 1$, the differential $D_{a_0}U(t,v)$ does not belong to $\mathscr{L}(L^1(\mathbb{R}^2))$ since the Gateaux-differential of the nonlinear operator N is not continuous from $L^1(\mathbb{R}^2)$ into $\mathscr{L}(L^1(\mathbb{R}^2))$.*

[3]Please, refer, for instance, to [20, p. 1] or [13, Section 3] for the definition of a nonlinear semigroup of operators.

We also stress that exact controllability results proved in Proposition 4.2 and Theorem 4.4 are quite general regarding assumptions on the connectivity kernel ω and the nonlinear response function f. For the validity of Proposition 4.2, it suffices that $\omega \in L^1(\mathbb{R}^2)$ to guarantee the existence of a unique solution to Equation (29). While for the validity of Theorem 4.4, it suffices that $\omega \in L^1(\mathbb{R}^2) \cap L^p(\mathbb{R}^2)$ and $f \in C^2(\mathbb{R})$ is bounded with its first and second derivatives, as it is sufficient for the validity of Lemma (B.8) (see, for instance, inequalities (111) and (116)).

5. On the visual MacKay effect modelling

As mentioned in the introduction, we stress that the physical visual stimuli employed in MacKay's experiments consist of funnel and tunnel patterns with highly localized information. Taking into account Equation (9) and the retino-cortical map, we incorporate these patterns as sensory inputs in Equation (NF), such that $I \in \{P_F, P_T\} + \varepsilon v$, where $\varepsilon > 0$ and v represents a localized function in the cortical domain intended to model the highly localized information present in the funnel and tunnel patterns. In this context, the function v can also be regarded as a localized distributed control, aiming to disrupt the *global* plane Euclidean symmetry of the funnel or tunnel pattern.

In Section 5.1, assuming that the response function f is linear, we provide a more general result showing that spontaneous cortical patterns cannot induce illusory contours in the output pattern. In particular, we deduce that $I \in \{P_F, P_T\}$ cannot induce the MacKay effect using Equation (NF). Then, using MacKay's stimuli $I \in \{P_F, P_T\} + \varepsilon v$, we prove in Section 5.2 that the linearized form of (NF) is sufficient to replicate the visual MacKay effect theoretically. Thus, the phenomenon starts in the linear regime, so the effect of saturating f should only dampen out high oscillations in the system. Section 5.3 provides theoretical proof of all these results when the response function f is a nonlinear sigmoid function.

5.1. **A priori analysis.**

In this section, we prove that it is necessary to break the Euclidean symmetry of funnel and tunnel pattern by localized control function for modelling the visual MacKay effect with Equation (NF), both with a linear and nonlinear response function. Our first result is the following.

Theorem 5.1. *Let $a_0 \in L^\infty(\mathbb{R}^2)$ and $I \in L^\infty(\mathbb{R}^2)$ given by $I(\cdot) = \cos(2\pi\langle \xi_0, \cdot \rangle)$, for some $\xi_0 \in \mathbb{R}^2$. Assume that the response function f is linear. If $\mu < \mu_0$, it holds*

$$a(\cdot, t) \xrightarrow[t\to\infty]{} \frac{I(\cdot)}{1 - \mu\widehat{\omega}(\xi_0)}, \qquad \text{exponentially in} \qquad L^\infty(\mathbb{R}^2), \tag{40}$$

where $a \in X_\infty$ is the solution of (NF) with initial datum a_0.

Proof. The stationary state associated with $I(\cdot) = \cos(2\pi\langle \xi_0, \cdot \rangle)$ is given by $a_I(\cdot) = I(\cdot)/(1 - \mu\widehat{\omega}(\xi_0))$. Indeed, one has for $x \in \mathbb{R}^2$,

$$I(x) + \mu(\omega * a_I)(x) = I(x) + \frac{\mu}{1 - \mu\widehat{\omega}(\xi_0)}(\omega * I)(x) = \frac{I(x)}{1 - \mu\widehat{\omega}(\xi_0)} = a_I(x), \tag{41}$$

since $\omega * I = \widehat{\omega}(\xi_0) I$. Therefore, if $\mu < \mu_0$, the result follows by the uniqueness of stationary state and exponential convergence of a to a_I in the space $L^\infty(\mathbb{R}^2)$ provided by Theorem 3.3. □

Corollary 5.2. *Assume that the response function f is linear. If $\mu < \mu_0$, then a_F (resp. a_P) is a funnel (resp. tunnel) pattern in shape as P_F (resp. P_T). In particular, Equation (NF) with a linear response function cannot reproduce the MacKay effect starting with a sensory input equal to P_F or P_T.*

Proof. Due to Theorem 5.1, the stationary states associated with P_F and P_T are respectively proportional to P_F and P_T so that they have the same binary pattern respectively (see, Section 2.2), and then the same geometrical shape in terms of images. □

We provide a similar result as that of Theorem 5.1 with the nonlinear function f in Equation (SS). This result shows, in particular, that even in the presence of the nonlinearity, Equation (NF) cannot describe the MacKay effect when the sensory input is chosen equal to P_F or P_T. Given that P_F and P_T have symmetrical roles, we focus only on P_F. We recall that they are analytically given in Cartesian cortical coordinates in V1 by (9).

Theorem 5.3. *Assume that the sensory input in Equation (SS) is taken as $I = P_F \in L^\infty(\mathbb{R}^2)$. If $\mu < \mu_0$, then the stationary state $a_F := \Psi(P_F) \in L^\infty(\mathbb{R}^2)$ associated with P_F explicitly depends solely upon x_2. Moreover, one has the following.*

1. *The function a_F is even and $1/\lambda$-periodic with respect to x_2;*
2. *The function a_F is infinitely differentiable, and Lipshitz continuous;*
3. *If in addition $\mu < \mu_0/2$ and the function f is odd, then a_F has a discrete and countable number of zeroes with respect to x_2, identical with that of $x_2 \mapsto \cos(2\pi\lambda x_2)$ on $\mathbb{R}$.*

Remark 5.4. *Notice the assumption $\mu < \mu_0/2$ in item 3. of Theorem 5.3 instead of $\mu < \mu_0$. We think this is a technical assumption because of the strategy used in our proof since numerical results suggest that item 3. remains valid for all $\mu < \mu_0$. Moreover, the assumption on the parity of f is also technical, and we conjecture that if f is not odd, then a_F will still have a discrete and countable number of zeroes with respect to x_2, such that*

$$a_F^{-1}(\{0\}) = \mathbb{R} \times \left\{ z_k \in \left] \frac{k}{2\lambda}, \frac{k+1}{2\lambda} \right[\mid k \in \mathbb{Z} \right\}, \tag{42}$$

and, for all $k \in \mathbb{Z}$,

$$|z_k - \tau_k| \leq \frac{\arcsin(\mu\mu_0^{-1})}{2\pi\lambda}, \qquad \text{where} \qquad \tau_k := \frac{2k+1}{4\lambda}. \tag{43}$$

The gap between the zeroes of a_F and those of P_F provided by (43) shows that on each interval, z_k and τ_k become arbitrarily close depending on whether μ is not closed to μ_0. Nevertheless, if λ is taken sufficiently large, z_k and τ_k become arbitrarily close independently of $\mu_0 - \mu$.

Proof of Theorem 5.3. We assume that $\lambda = 1$ in the sequel for ease of notation. We know by item *3.* of Proposition A.3 that if P_F or a_F has a subgroup of $\mathbf{E}(2)$ as a group of symmetry, the other has the same subgroup as a group of symmetry and conversely. Since $P_F(x_1, x_2)$ is independent on x_1, it follows that $a_F(x_1, x_2)$ is also independent on x_1 for all $(x_1, x_2) \in \mathbb{R}^2$. Similarly, since P_F is invariant under the action of the reflection with respect to the straight $x_1 = 0$, that is, $P_F(x_1, -x_2) = P_F(x_1, x_2)$ for all $(x_1, x_2) \in \mathbb{R}^2$, one deduces that $a_F(x_1, -x_2) = a_F(x_1, x_2)$. Thus, a_F is an even function with respect to x_2. Similarly, since P_F is invariant under the translation by vector $(0, -1) \in \mathbb{R}^2$, it follows that a_F is also invariant under this translation so that a_F is 1-periodic with respect to x_2. The fact that a_F is infinitely differentiable on $\mathbb{R}^2$ follows immediately from that $P_F \in C^\infty(\mathbb{R}^2)$, the kernel $\omega \in \mathcal{S}(\mathbb{R}^2) \subset C^\infty(\mathbb{R}^2) \cap L^1(\mathbb{R}^2)$ and that f is bounded. Writing now $a_F(x_2) := a_F(x_1, x_2)$ for notational ease, we obtain that a_F is also given by

$$a_F(x_2) = \cos(2\pi x_2) + \mu[\omega_1 * f(a_F)](x_2), \qquad x_2 \in \mathbb{R}, \tag{44}$$

where ω_1 is a 1D difference of Gaussian kernel . Let $a_F' := \partial_{x_2} a_F$, then due to (44), one obtains

$$a_F'(x_2) = -2\pi \sin(2\pi x_2) + \mu[\omega_1' * f(a_F)](x_2), \qquad x_2 \in \mathbb{R}. \tag{45}$$

Since $\|f\|_\infty \leq 1$ by assumption, it follows that $\|a_F'\|_\infty \leq 2\pi + \mu\|\omega_1'\|_1 < \infty$. Therefore, a_F is Lipschitz continuous.

We now present an argument to prove item *3.* of Theorem 5.3. Notice that $a_F = \Psi(P_F)$ satisfies

$$a_F = P_F + \mu\omega * f(a_F). \tag{46}$$

Let $x^* := (x_1^*, x_2^*) \in \mathbb{R}^2$ be such that $P_F(x^*) = 0$. It follows from (46) that

$$a_F(x^*) = \mu \int_{\mathbb{R}^2} \omega(y) f(a_F(x^* - y))dy. \tag{47}$$

By using (46) once again, one obtains

$$a_F(x^* - y) = \cos(2\pi(x_2^* - y_2)) + \mu \int_{\mathbb{R}^2} \omega(y - z) f(a_F(x^* - z))dz. \tag{48}$$

We introduce the map $g_3 : y := (y_1, y_2) \in \mathbb{R}^2 \longmapsto g_3(y) := a_F(x^* - y)$. Then, it is straightforward to observe that, g_3 is the unique solution of (48) for every $\mu < \mu_0$, and it holds

$$-a_F(x^* + y) = \cos(2\pi(x_2^* - y_2)) + \mu \int_{\mathbb{R}^2} \omega(y - z) f(-a_F(x^* + z))dz,$$

since f is odd. So the function $y \in \mathbb{R}^2 \mapsto -g_3(-y)$ is also solution of (48). By uniqueness of solution, one has $g_3(-y) = -g_3(y)$ and that $y \in \mathbb{R}^2 \longmapsto \omega(y) f(a_F(x^* - y))$ is an odd function, since ω is symmetric and f is and odd function. It follows that the right-hand side of (47) is equal to 0.

To show the converse inclusion, let $x^* := (x_1^*, x_2^*) \in \mathbb{R}^2$ verifying $a_F(x^*) = 0$. From (46), it follows

$$\cos(2\pi x_2^*) = -\mu \int_{\mathbb{R}^2} \omega(y) f(a_F(x^* - y))dy. \tag{49}$$

Developing $\cos(2\pi(x_2^* - y_2))$ and replacing in (48) $\cos(2\pi x_2^*)$ by its expression in (49), one obtains for $y \in \mathbb{R}^2$,

$$a_F(x^* - y) = \sin(2\pi x_2^*)\sin(2\pi y_2) + \mu \int_{\mathbb{R}^2} k(y, z) f(a_F(x^* - z))dz, \tag{50}$$

where $k(y, z) := \omega(y - z) - \cos(2\pi y_2)\omega(z)$, satisfies

$$K := \sup_{y \in \mathbb{R}^2} \int_{\mathbb{R}^2} |k(y, z)|dy \leq 2\|\omega\|_1. \tag{51}$$

Since $\mu < \mu_0/2$, the contracting mapping principle shows that for every $I \in L^\infty(\mathbb{R}^2)$ there exists a unique solution $b \in L^\infty(\mathbb{R}^2)$ to

$$b(y) = I(y) + \mu \int_{\mathbb{R}^2} k(y, z) f(b(z))dz. \tag{52}$$

By (50), function $b(y) := a_F(x^* - y)$ is the unique solution of the above equation associated with $I(y) = \sin(2\pi x_2^*)\sin(2\pi y_2)$.

On the other hand, since ω is symmetric and the sigmoid f is an odd function, we have also for a. e., $y \in \mathbb{R}^2$,

$$-a_F(x^* + y) = \sin(2\pi x_2^*)\sin(2\pi y_2) + \mu \int_{\mathbb{R}^2} k(y, z) f(-a_F(x^* + z))dz, \tag{53}$$

so that, the function $\tilde{b}(y) = -b(-y)$ is also solution of Equation (52) associated with the input $I(y) = \sin(2\pi x_2^*)\sin(2\pi y_2)$. By uniqueness of solution, one then has $b(-y) = -b(y)$ for a. e., $y \in$

$\mathbb{R}^2$. This shows that $y \mapsto \omega(y) f(a_F(x^* - y))$ is an odd function on $\mathbb{R}^2$, since ω is symmetric and f is an odd function, which implies that the r.h.s. of (49) is equal to 0 and thus that $x^* \in P_F^{-1}(\{0\})$. □

The proof of the following corollary follows the same lines as that of Corollary 5.2.

Corollary 5.5. *Under assumption, $\mu < \mu_0$, a_F (resp. a_T) is a funnel (resp. tunnel) pattern in shape. In particular, Equation (NF) with a sigmoid activation function cannot reproduce the MacKay effect starting with a sensory input equal to P_F or P_T.*

Remark 5.6. *By following the lines in the proof of Theorem 5.3, we can notice that it is only sufficient for the kernel ω to be homogeneous and isotropically invariant to obtain the desired results.*

5.2. **The visual MacKay effect with a linear response function.** The results we provide in this section aim to replicate the MacKay effect using Equation (NF) when the response function f is linear. The Corollary 5.2 shows that, for our model of cortical activity in V1, one cannot obtain the MacKay effect in the linear regime without breaking the Euclidean plane symmetry of the sensory input when chosen equal to P_F or P_T. Our purpose now is to show that Equation (NF) with the linear response function and sensory input $I \in \{P_F, P_T\} + \varepsilon v$ reproduces the MacKay effect. Here, v is a suitable control function that should model the localized information in MacKay's stimuli.

Remark 5.7. *We notice that only the description of the MacKay effect related to the funnel pattern will be shown for ease of presentation and reader convenience. Then, in the rest of this section, we focus on describing the MacKay effect related to the "MacKay rays"; see Fig 1.*

One of the essential characteristics of the retino-cortical map, i.e. the way the visual field is projected into V1, is that small objects located in the fovea, which is the center of the visual field, have a much more extensive representation in V1 than similar objects located in the peripheral visual field. As a result, for the cortical representation of the "MacKay rays" visual stimulus, we choose a sensory input in Equation (NF) as $I(x) = P_F(x) + \varepsilon H(\theta - x_1)$, where $\varepsilon > 0$, $\theta \in \mathbb{R}$ and H is the Heaviside step function. This choice models the highly localized information in the center of the funnel pattern *created by the very fast alternation of black and white rays*. It is worth noting that this corresponds to localized information in horizontal stripes in the left area of the cortex.

To keep the presentation as clear as possible for reader convenience, we let $\theta = 0$, and we assume that the cortical representation of the "MacKay rays" visual stimulus is given by

$$I(x) = \cos(2\pi\lambda x_2) + \varepsilon H(-x_1), \qquad \lambda,\ \varepsilon > 0,\ x := (x_1, x_2) \in \mathbb{R}^2. \tag{54}$$

The sensory input $v(x_1, x_2) = H(-x_1)$ is dependent only on the variable x_1. As a result of Remark A.4, the associated stationary output b is also dependent solely on that variable. Therefore, our current task is to compute the solution b of the following equation

$$b(x) = I(x) + \mu(\omega_1 * b)(x), \qquad x \in \mathbb{R}, \tag{55}$$

where $I(x) = H(-x)$ and the 1-D kernel ω_1 is given by

$$\omega_1(x) = [\sigma_1\sqrt{2\pi}]^{-1} e^{-\frac{x^2}{2\sigma_1^2}} - \kappa[\sigma_2\sqrt{2\pi}]^{-1} e^{-\frac{x^2}{2\sigma_2^2}}, \qquad x \in \mathbb{R}. \tag{56}$$

$$\widehat{\omega_1}(\xi) = e^{-2\pi^2\sigma_1^2\xi^2} - \kappa e^{-2\pi^2\sigma_2^2\xi^2}. \tag{57}$$

Lemma 5.8. *Let $I \in \mathcal{S}'(\mathbb{R})$ and the kernel $\omega_1 \in \mathcal{S}(\mathbb{R})$ be defined by (56). Under the assumption $\mu < \mu_c$, there is a unique solution $b \in \mathcal{S}'(\mathbb{R})$ to Equation (55), which is given by*

$$b = I + \mu K * I. \tag{58}$$

Here the kernel $K \in \mathcal{S}(\mathbb{R})$ is defined of all $x \in \mathbb{R}$ by

$$K(x) = \int_{-\infty}^{+\infty} e^{2i\pi\xi x}\widehat{K}(\xi)d\xi, \qquad \text{where} \qquad \widehat{K}(\xi) = \frac{\widehat{\omega_1}(\xi)}{1-\mu\widehat{\omega_1}(\xi)}, \qquad \forall \xi \in \mathbb{R}. \tag{59}$$

Proof. First of all, under assumptions on I and ω_1, we have that Equation (55) is well-posed in $\mathcal{S}'(\mathbb{R})$. Then taking respectively the Fourier transform of (55) and the inverse Fourier transform in the space $\mathcal{S}'(\mathbb{R})$, we find that $b \in \mathcal{S}'(\mathbb{R})$ is given by (58) with $K \in \mathcal{S}(\mathbb{R})$ defined as in (59). Indeed, observe that $\widehat{K}$ is well-defined on $\mathbb{R}$ due to hypothesis $\mu < \mu_c$, with μ_c being defined in (1), and it belongs to the Schwartz space $\mathcal{S}(\mathbb{R})$ as the product of a $C^\infty(\mathbb{R})$ function and an element of $\mathcal{S}(\mathbb{R})$. □

Due to Lemma 5.8, inverting the kernel K defined in (59) and providing an asymptotic behaviour of its zeroes on $\mathbb{R}$ will help to provide detailed information on the qualitative properties of the function b as given by (58). To achieve this, we use tools from complex.

Let us consider the extension of $\widehat{K}$ in the set $\mathbb{C}$ of complex numbers,

$$\widehat{K}(z) = \frac{\widehat{\omega_1}(z)}{1-\mu\widehat{\omega_1}(z)}, \qquad z \in \mathbb{C}. \tag{60}$$

Then $\widehat{K}$ is a meromorphic function on $\mathbb{C}$, and its poles are zeroes of the entire function

$$h(z) := 1 - \mu e^{-2\pi^2\sigma_1^2 z^2} + \kappa\mu e^{-2\pi^2\sigma_2^2 z^2}, \qquad z \in \mathbb{C}. \tag{61}$$

Remark 5.9. *The holomorphic function h is an exponential polynomial [2, Chapter 3] in $-z^2$ with frequencies $\alpha_0 = 0$, $\alpha_1 = 2\pi^2\sigma_1^2$ and $\alpha_2 = 2\pi^2\sigma_2^2$ satisfying $\alpha_0 < \alpha_1 < \alpha_2$ due to assumptions on σ_1 and σ_2. It is normalized since the coefficient of 0-frequency equals 1. A necessary condition for h for being factorizable [2, Remark 3.1.5, p. 201] is that parameters σ_1 and σ_2 are taken so that it is simple. By definition [2, Definition 3.1.4, p. 201], h is simple if α_1 and α_2 are commensurable, i.e., $\alpha_1/\alpha_2 \in \mathbb{Q}$, which is equivalent to $\sigma_1^2/\sigma_2^2 \in \mathbb{Q}$. Here $\mathbb{Q}$ denote the set of rational numbers.*

Remark 5.10. *For ease in computation and pedagogical presentation, we assume in the rest of this section that parameters in the kernel ω defined in (4) and then in the 1-D kernel ω_1 defined in (56) are given by $\kappa = 1$, $2\pi^2\sigma_1^2 = 1$ and $2\pi^2\sigma_2^2 = 2$. In this case, one has $\mu_0 := \|\omega\|_1^{-1} = 2$ and $\mu_c := \widehat{\omega}(\xi_c)^{-1} = 4$. In particular ω satisfies the balanced condition $\widehat{\omega}(0) = 0$. Then, assuming in this particular consideration that $\mu := 1 < \mu_0 = 2$ is not a loss of generality.*

The main result of this section is then the following.

Theorem 5.11. *Assume that the response function f is linear and the input I is given by (54). Under the considerations of Remark 5.10, the unique stationary state to Equation (NF) is given for all $(x_1, x_2) \in \mathbb{R}^2$ by*

$$a_I(x_1, x_2) = \frac{\cos(2\pi\lambda x_2)}{1-\mu\widehat{\omega}(\xi_0)} + \varepsilon g(x_1), \qquad \xi_0 := (0, \lambda), \tag{62}$$

where $g : \mathbb{R} \to \mathbb{R}$ has a discrete and countable set of zeroes on $(0, +\infty)$.

Observe that under the assumption that the response function f is linear, Equation (NF) becomes linear. It follows that the first term in the r.h.s. of (62) is the stationary output associated with the input P_F by using Theorem 5.1, and b is the stationary output associated with the sensory input $v(x_1, x_2) = H(-x_1)$. Consequently, Theorem 5.11 follows from the following proposition. The proof is an immediate consequence of Lemma 5.8, Theorem B.1 and Proposition B.4 given in Section B.1.

Proposition 5.12. *Let $I(x) = H(-x)$, $x \in \mathbb{R}$, H being the Heaviside step function. Under the considerations of Remark 5.10, the solution $b \in L^\infty(\mathbb{R})$ of (55) is given, for $x > 0$, by*

$$e^{\pi x\sqrt{\frac{2\pi}{3}}} b(x) = \frac{\sqrt{3}}{\pi} \cos\left(\frac{\pi}{3} + \pi x\sqrt{\frac{2\pi}{3}}\right) + O\left(\frac{1}{x}\right). \tag{63}$$

Moreover, letting $(\theta_k)_{k\in\mathbb{N}^*}$ and $(\tau_k)_{k\in\mathbb{N}^*}$ be respectively zeroes and extrema of $x \mapsto \cos(\pi/3 + \pi x\sqrt{2\pi/3})$ for $x > 0$, the zeroes of b in $(0, +\infty)$ are a countable sequence $(\rho_k)_{k\in\mathbb{N}^*}$ such that ρ_k is unique in the interval $J_k :=]\tau_k, \tau_{k+1}[$ for all $k \in \mathbb{N}^*$ and it holds

$$|\theta_{k+1} - \rho_k| \leq \frac{\sqrt{6}}{2\pi^2} \arcsin\left(\frac{2\sqrt{5}}{5\pi(3k-1)}\right), \qquad \forall k \in \mathbb{N}^*. \tag{64}$$

Proof. If $I(x) = H(-x)$, $x \in \mathbb{R}$, is the input in Equation (55), then by Lemma 5.8 and Theorem B.1, the solution $b \in L^\infty(\mathbb{R})$ of (55) is given for all $x > 0$ by

$$\begin{aligned} \frac{b(x)}{2\sqrt{\pi}} &= \int_x^{+\infty} e^{-\pi y\sqrt{\frac{2\pi}{3}}} \cos\left(\frac{\pi}{12} + \pi y\sqrt{\frac{2\pi}{3}}\right) dy \\ &\quad + \int_x^{+\infty} \sum_{k=1}^{+\infty} \frac{e^{-\pi c_k y\sqrt{\frac{2\pi}{3}}}}{c_k} \cos\left(\frac{\pi}{12} + \pi c_k y\sqrt{\frac{2\pi}{3}}\right) dy \\ &\quad + \int_x^{+\infty} \sum_{k=1}^{+\infty} \frac{e^{-\pi d_k y\sqrt{\frac{2\pi}{3}}}}{d_k} \sin\left(\frac{\pi}{12} - \pi d_k y\sqrt{\frac{2\pi}{3}}\right) dy, \end{aligned} \tag{65}$$

where the sequences $(c_k)_k$ and $(d_k)_k$ are defined in (78). Since these two sequences are positives and tend to $+\infty$ as $k \to +\infty$, we can commute the integrals and the sums in the r.h.s of (65) for all $x > 0$. One finds,

$$\begin{aligned} b(x) &= \frac{\sqrt{3}}{\pi} \cos\left(\frac{\pi}{3} + \pi x\sqrt{\frac{2\pi}{3}}\right) e^{-\pi x\sqrt{\frac{2\pi}{3}}} + \frac{\sqrt{3}}{\pi} \sum_{k=1}^{+\infty} \frac{e^{-\pi c_k x\sqrt{\frac{2\pi}{3}}}}{c_k^2} \cos\left(\frac{\pi}{3} + \pi c_k x\sqrt{\frac{2\pi}{3}}\right) \\ &\quad - \frac{\sqrt{3}}{\pi} \sum_{k=1}^{+\infty} \frac{e^{-\pi d_k x\sqrt{\frac{2\pi}{3}}}}{d_k^2} \cos\left(\frac{\pi}{3} + \pi d_k x\sqrt{\frac{2\pi}{3}}\right), \end{aligned} \tag{66}$$

and (63) immediately follows. Finally, to prove (64), it suffices to repeat step by step the proof of Lemma B.3 and Proposition B.4 given in Section B.1. □

The Proposition 5.12 implies that if the sensory input is the V1 representation of the "MacKay rays" as defined by (54), then the associated stationary state corresponds to the V1 representation of the afterimage reported by MacKay [17]. Moreover, Theorem 3.3 ensures that the average membrane potential $a(x, t)$ of neurons in V1 located at $x \in \mathbb{R}^2$ at time $t \geq 0$ exponentially stabilises on the stationary state when $t \to \infty$. It follows that Equation (NF) theoretically replicates the MacKay effect associated with the "MacKay rays" at the cortical level. Due to

the retino-cortical map between the visual field and V1, we deduce the theoretical description of the MacKay effect for the "MacKay rays" at the retinal level.

Remark 5.13. *We emphasise that a linear combination of the Heaviside step function in the x_2-variable as a perturbation of the V1 representation of the tunnel pattern (called "MacKay target") gives rise to the MacKay effect description related to this pattern.*

While in the funnel pattern used in MacKay experiences, the difference between the center and the rest of the image is more evident, one must notice that the MacKay target stimulus (Figure 2, the right panel) is not perfectly radial. Indeed, symmetry-breaking imperfections are present. We chose to mimic these imperfections by shaping our control as concentrated on rays converging to the origin, which we chose to be symmetric for mathematical convenience (this has no bearing on the results). This control captures that a symmetry-breaking in the input is necessary to induce the observed afterimage and is sufficiently simple to be mathematically tractable. We stress that the effect of adding such rays is barely noticeable (see, e.g., the left panel in Figure 8, where the two rays are along the line passing horizontally through the center of the image).

5.3. **The visual MacKay effect with a nonlinear response function.** This section aims to show that Equation (NF) with a nonlinear response function f still replicates the MacKay effect associated with the "MacKay rays" and the "MacKay target", see Figure 2.

Remark 5.4 and Corollary 5.5 shows that, for our model of cortical activity in V1 modelled by Equation (NF), one cannot replicate the MacKay effect even with a nonlinear response function (having standard properties in most neural fields model, namely, a sigmoid) without breaking the Euclidean plane symmetry of the sensory input when chosen equal to P_F or P_T. In the following, in order to see why a response function with sigmoid shape replicates the MacKay effect, we assume the following hypothesis.

Hypothesis 5.14. *The response function f satisfies: $f \in C^2(\mathbb{R})$, f is odd and $f(s) = s$ for all $|s| \leq 1$. We also assume that* $\max_{s\in\mathbb{R}} f'(s) = 1$.

Let us model the cortical representation of the "MacKay rays" input by the following

$$I(x) = \gamma P_F(x) + \varepsilon H(-x_1), \qquad x := (x_1, x_2) \in \mathbb{R}^2, \tag{67}$$

where $\gamma \geq 0$ is a control parameter, $\varepsilon > 0$ and $P_F(x) = \cos(2\pi\langle \xi_0, x\rangle)$ is an analytical representation of the funnel pattern in cortical coordinates, where $\xi_0 = (0, \lambda)$ with $\lambda > 0$.

The first result of this section is then the following

Proposition 5.15. *Let the input I be defined by (67) with $\varepsilon > 0$ small and $\gamma \leq 1 - \mu\widehat{\omega}(\xi_0)$. Under the assumption, $\mu < \mu_0$, equation (NF) with a response function satisfying Hypothesis 5.14 replicates the MacKay effect associated with the "MacKay rays".*

Proof. On one hand, the stationary solution associated with $I(x) = \gamma P_F(x) + \varepsilon v(x_1, x_2)$, where $v(x_1, x_2) = H(-x_1)$ satisfies (24) in $L^\infty(\mathbb{R}^2)$, i.e.,

$$\Psi(\gamma P_F + \varepsilon v) = \gamma P_F + \varepsilon v + \mu\omega * f(\Psi(\gamma P_F + \varepsilon v)). \tag{68}$$

On the other hand, since $\|P_F\|_\infty = 1 = \|v\|_\infty$, $0 < \gamma \leq 1 - \mu\widehat{\omega}(\xi_0) \leq 1$ and $\varepsilon \ll 1$, we can apply Theorem B.7 and obtain

$$\Psi(\gamma P_F + \varepsilon v) = \Psi(\gamma P_F) + \varepsilon D\Psi(\gamma P_F)v + o(\varepsilon), \tag{69}$$

where $D\Psi(\gamma P_F)v$ is the differential of Ψ at γP_F in the direction of v. It also follows from Theorems 3.3 and B.6 that for some $g_1 \geq 0$, it holds $\|\Psi(\gamma P_F)\|_\infty \leq g_1 = \gamma\|P_F\|_\infty + (\mu/\mu_0)f(g_1) < 3/2$.

Thus, injecting (69) into (68) and Taylor expansion of f in the first order leads to

$$\Psi(\gamma P_F) = \gamma P_F + \mu\omega * f(\Psi(\gamma P_F)), \quad D\Psi(\gamma P_F)v = v + \mu\omega * [f'(\Psi(\gamma P_F))D\Psi(P_F)v.] \tag{70}$$

Thanks to Hypothesis 5.14 and the assumption $\gamma \leq 1 - \mu\widehat{\omega}(\xi_0)$, one has $\Psi(\gamma P_F) = \gamma P_F/(1 - \mu\widehat{\omega}(\xi_0))$. Indeed, since $|\gamma P_F/(1 - \mu\widehat{\omega}(\xi_0)| \leq 1$ and $\omega * P_F = \widehat{\omega}(\xi_0)P_F$, one has that

$$\gamma P_F + \mu\omega * f\left(\frac{\gamma P_F}{1 - \mu\widehat{\omega}(\xi_0)}\right) = \gamma P_F + \frac{\mu\gamma\omega * P_F}{1 - \mu\widehat{\omega}(\xi_0)} = \frac{\gamma P_F}{1 - \mu\widehat{\omega}(\xi_0)}. \tag{71}$$

Therefore, $\Psi(\gamma P_F)$ is also a funnel pattern when represented in term of binary image. Moreover, since $|\Psi(\gamma P_F)| \leq 1$, one has $f'(\Psi(\gamma P_F)) = 1$, and $D\Psi(\gamma P_F)v = v + \mu\omega * D\Psi(P_F)v$ has a discrete and countable set of zeroes by Proposition 5.12. The result then follows at once. □

Proposition 5.16. *Let $v \in L^\infty(\mathbb{R}^2)$. Under the assumption $\mu < \mu_0$, the map $\Pi : \gamma \in \mathbb{R}_{\geq 0} \mapsto \Pi(\gamma) = u_\gamma \in L^\infty(\mathbb{R}^2)$, where u_γ is the solution of $u_\gamma = v + \mu\omega * [f'(\Psi(\gamma P_F))u_\gamma]$ is Lipschitz continuous.*

Proof. Let $v \in L^\infty(\mathbb{R}^2)$ be fixed and $\gamma \in \mathbb{R}_{\geq 0}$. If $u_\gamma \in L^\infty(\mathbb{R}^2)$ is the solution of $u_\gamma = v + \mu\omega * [f'(\Psi(\gamma P_F))u_\gamma]$, then, under the assumption $\mu < \mu_0$ and Hypothesis 5.14, one has $\|u_\gamma\|_\infty \leq \|v\|_\infty\mu_0/(\mu - \mu_0)$. Let now $\gamma_1, \gamma_2 \in \mathbb{R}_{\geq 0}$, then using Inequality (25), one finds

$$\begin{aligned} \|\Pi(\gamma_1) - \Pi(\gamma_2)\|_\infty &\leq \mu\|\omega\|_1\|f'(\Psi(\gamma_1 P_F))u_{\gamma_1} - f'(\Psi(\gamma_2 P_F))u_{\gamma_2}\|_\infty \\ &\leq \frac{\mu}{\mu_0}\|\Pi(\gamma_1) - \Pi(\gamma_2)\|_\infty + \frac{\mu\mu_0\|v\|_\infty f''_\infty}{(\mu_0 - \mu)^2}|\gamma_1 - \gamma_2|, \end{aligned} \tag{72}$$

where f''_∞ is the L^∞-norm of the second derivative f''. The result then follows at once. □

Let us define the positive quantity

$$\gamma_0 := \sup\{\gamma \geq 0 \mid \|\Psi(\gamma' P_F)\|_\infty \leq 1, \text{for all } \gamma' \in [0, \gamma]\}. \tag{73}$$

Observe that γ_0 is not necessary finite and that if $0 \leq \gamma \leq \gamma_0$, then $f'(\Psi(\gamma P_F)) = 1$. It follows that if $\gamma_0 = +\infty$, then $\|\Psi(\gamma P_F)\|_\infty \leq 1$ for all $\gamma \geq 0$ and therefore, under Assumption $\mu < \mu_0$, Equation (NF) with a response function satisfying Hypothesis 5.14 and with the input I defined by (67) with $\varepsilon > 0$ will always reproduce the MacKay effect associated with "MacKay rays" thanks to Proposition 5.16.

In the case where γ_0 is finite, one has the following.

Theorem 5.17. *Let $L > 0$. If γ_0 defined by (73) is finite, there exists $\delta > 0$ such that the stationary solution to Equation (NF) with a response function satisfying Hypothesis 5.14 and with the input I defined by (67) with $\varepsilon > 0$ small and $|\gamma - \gamma_0| \leq \delta$ has the same zeroes structure as in the linear case in $[0, L] \times \mathbb{R}$, under Assumption $\mu < \mu_0$. In particular, it replicates the MacKay effect associated with the "MacKay rays".*

Proof. Let $\varepsilon > 0$ be small and γ_0 defined by (73) be finite. On one hand, by definition of γ_0 and Proposition 5.15, the stationary solution $a_I(x_1, x_2)$ to Equation (NF) with a response function satisfying Hypothesis 5.14 and with the input I defined by (67) with $\gamma = \gamma_0$ has a discrete and countable zero-level set with respect to each of its variables $x_1 > 0$ and $x_2 \in \mathbb{R}$. On the other hand, one has for all $\gamma \geq 0$, $\Psi(\gamma P_F + \varepsilon v) = \Psi(\gamma P_F) + \varepsilon u_\gamma + o(\varepsilon)$ where $u_\gamma \in L^\infty(\mathbb{R}^2)$ is the solution of $u_\gamma = v + \mu\omega * [f'(\Psi(\gamma P_F))u_\gamma]$. We known from Theorems 5.1 and 5.3 that $\Psi(\gamma P_F)$ has a discrete set of zeroes with respect to x_2 as P_F, and from Proposition 5.16 that for all $\eta > 0$, there exists $\delta > 0$ such that, if $|\gamma - \gamma_0| \leq \delta$ it holds $\|u_\gamma - u_{\gamma_0}\|_\infty \leq \eta$. Therefore, since u_{γ_0} has a discrete set of zeroes with respect to $x_1 > 0$, then the zeroes of the function u_γ cannot

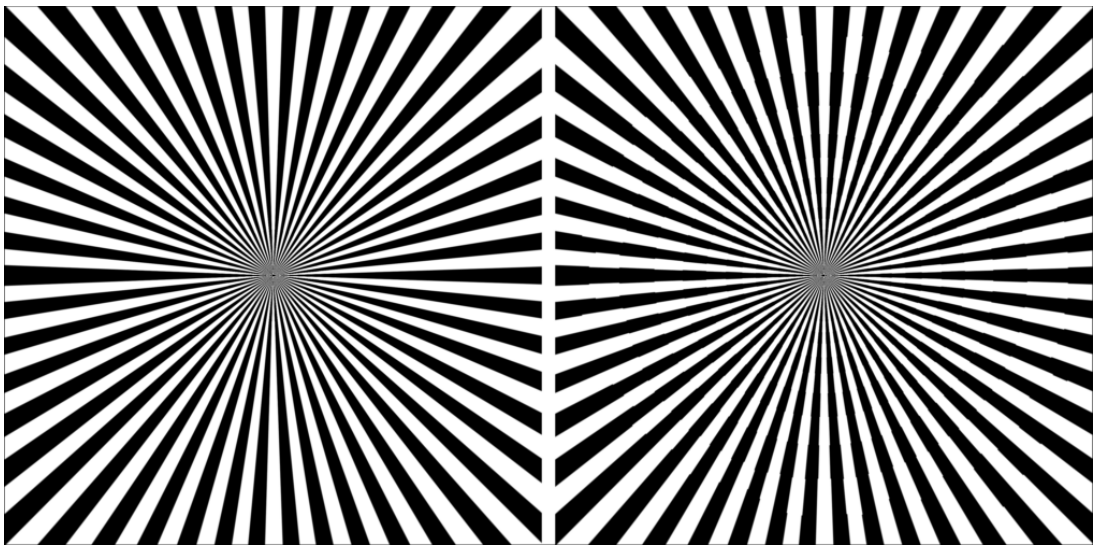

FIGURE 5. MacKay effect (*right*) on the "MacKay rays" (*left*). We use the linear response function $f(s) = s$. The sensory input is chosen as $I(x) = \cos(5\pi x_2) + \varepsilon H(2 - x_1)$, $\varepsilon = 0.025$, where H is the Heaviside step function.

accumulate at any of those zeroes in a finite interval, that is, the zeroes of both functions are distributed similarly in $[0, L] \times \mathbb{R}$ for all finite $L > 0$. □

Remark 5.18. *Although a sigmoid nonlinearity such as* $f(s) = \tanh(s)$ *or* $f(s) = \operatorname{erf}(s\sqrt{\pi}/2)$ *does not satisfy the assumption* $f(s) = s$ *for* $|s| \leq 1$*, it is almost linear in a small interval of the form* $(-\varepsilon, \varepsilon)$*,* $\varepsilon > 0$ *in such a way that Theorem 5.17 should be a theoretical explanation of why Equation* (NF) *with this nonlinearity replicates the MacKay effect.*

5.4. **Numerical results for the visual MacKay effect.** The numerical implementation is performed with Julia, where we coded retino-cortical map for visualising each experiment. Moreover, given a sensory input I, the associated stationary output a_I is numerically implemented via an iterative fixed-point method. Following the convention adopted in [8, 4] for geometric visual hallucinations, we present binary versions of these images, where black corresponds to positive values and white to negative ones as explained in Section 2.2. The reader may refer to [25, Appendix B] for a toolbox that performs numerical results presented here.

The cortical data is defined on a square $(x_1, x_2) \in [-L, L]^2$, $L = 10$ with steps $\Delta x_1 = \Delta x_2 = 0.01$. For the reproduction of the MacKay effect, parameters in the kernel ω given by (4) are $\kappa = 1$, $2\pi^2\sigma_1^2 = 1$, and $2\pi^2\sigma_2^2 = 2$. We also choose $\mu := 1$. We collected some representative results in Figures 5, 6, 7 and 8. Here, we visualize the retinal representation obtained from the cortical patterns via the inverse retino-cortical map. In Figure 5, we exhibit the MacKay effect associated with the "MacKay rays". In this case, the sensory input is chosen as $I(x) = \cos(5\pi x_2) + \varepsilon H(2 - x_1)$, where $\varepsilon = 0.025$ and H being the Heaviside step function. Similarly, we exhibit in Figure 6 the MacKay effect associated with the "MacKay target". In this case, the sensory input is $I(x) = \cos(5\pi x_1) + \varepsilon(H(-x_2 - 9.75) + H(x_2 - 9.75) + H(0.25 - |x_2|))$, where $\varepsilon = 0.025$ and H being the Heaviside step function. We use a linear response function ($f(s) = s$) for the two figures. However, the phenomenon can be reproduced with any sigmoid function. See for instance, Figure 7 and Figure 8.

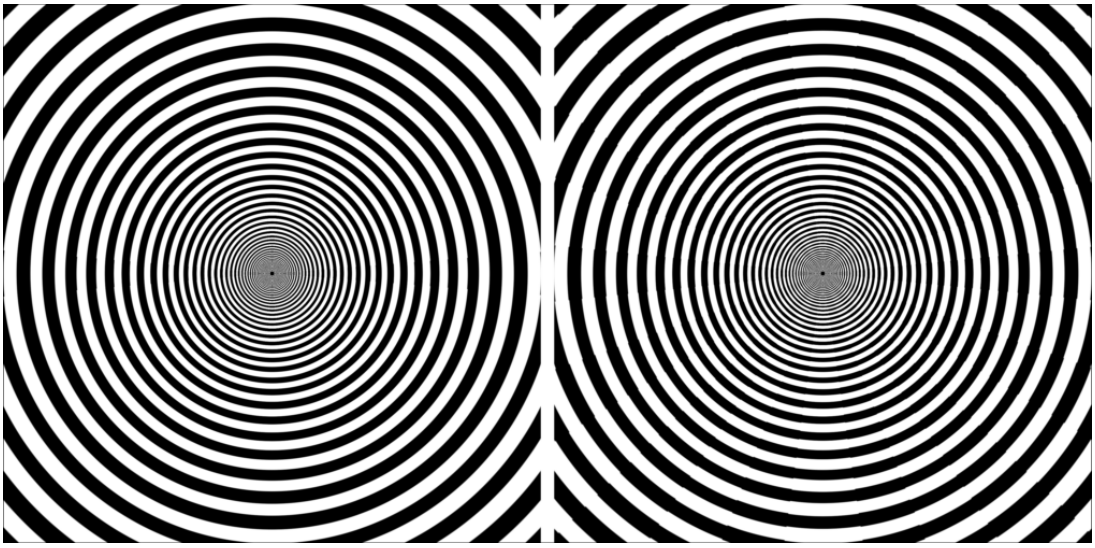

FIGURE 6. MacKay effect (*right*) on the "MacKay target" (*left*).We use the linear response function $f(s) = s$. The sensory input is $I(x) = \cos(5\pi x_1) + \varepsilon(H(-x_2 - 9.75) + H(x_2 - 9.75) + H(0.25 - |x_2|))$, $\varepsilon = 0.025$, where H is the Heaviside step function.

Remark 5.19. *Although the Gaussian kernel is usually used in image processing and computer vision tasks due to its proximity to the visual system, it cannot replicate the MacKay effect if we use it as the kernel in Equation* (NF)*. A physiological reason for this is that we used a one-layer model of NF equations. It is not then biologically realistic to model synaptic interactions with a Gaussian, which would model only excitatory-type interactions between neurons, see also Remark B.5.*

6. Discussion

In this paper, we investigated the replication of visual illusions reported by MacKay [17], referred to as the visual MacKay effect. We have shown that these intriguing visual phenomena can be theoretically explained through a neural field model of Amari-type modelling the average membrane potential of V1 spiking neurons, which takes into account the sensory input from the retina. In our model equation, the sensory input stands to the V1 representation via the retino-cortical map of the visual stimulus employed in the MacKay experiment. Assuming that the intra-neuron connectivity parameter is smaller than the threshold parameter where cortical patterns spontaneously emerge in V1 when sensory inputs from the retina do not drive its activity, we expounded a mathematical sound framework consisting of the input-output controllability of this equation. Then, performing a quantitative and qualitative study of the stationary output, we found that the MacKay effect is essentially a linear phenomenon, meaning the non-linear nature of the neural response does not play a role in its replication via our model equation.

Although our approach differs from that of Nicks *et al.* [19] in describing the MacKay-like effect (associated with regular sensory input), it agrees with the latter in emphasizing the role of inhibitory neurons in shaping the response of excitatory neurons to visual stimuli.

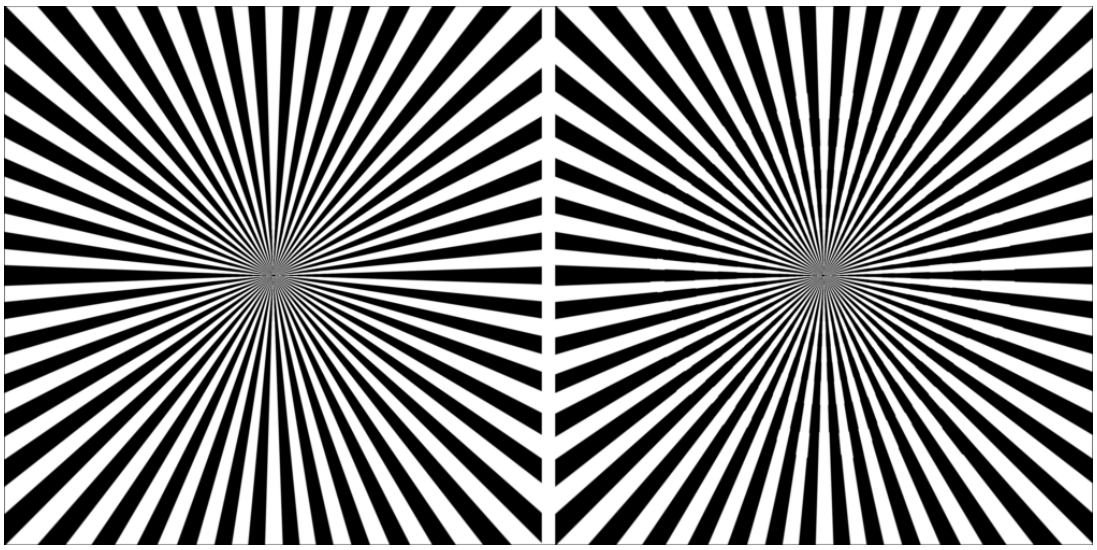

FIGURE 7. MacKay effect (*right*) on the "MacKay rays" (*left*). We use the nonlinear response function $f(s) = s/(1+|s|)$. The sensory input is chosen as $I(x) = \cos(5\pi x_2) + \varepsilon H(2 - x_1)$, $\varepsilon = 0.025$, where H is the Heaviside step function.

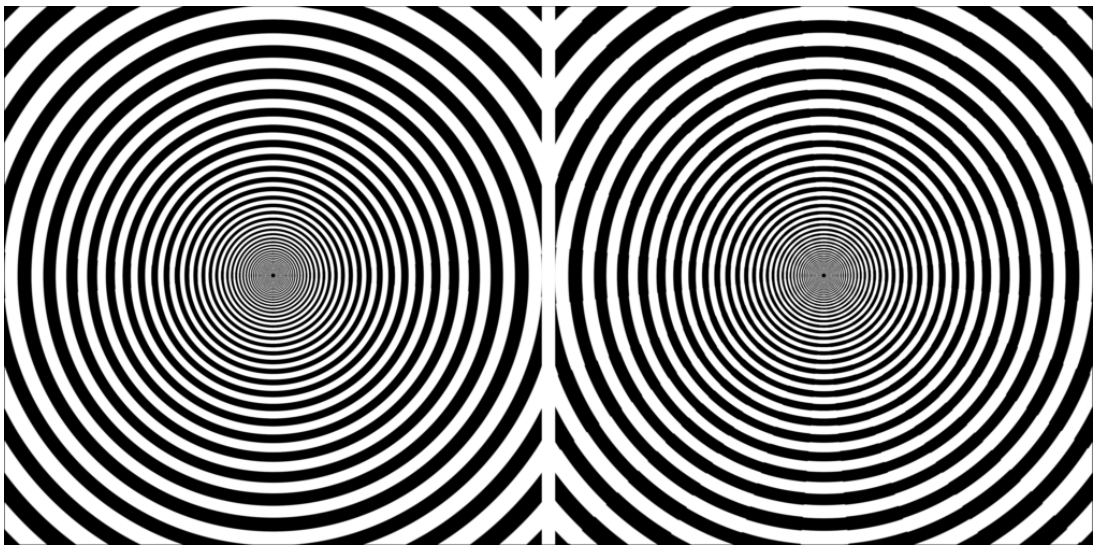

FIGURE 8. MacKay effect (*right*) on the "MacKay target" (*left*).We use the nonlinear response function $f(s) = s/(1+|s|)$. The sensory input is $I(x) = \cos(5\pi x_1) + \varepsilon(H(-x_2 - 9.75) + H(x_2 - 9.75) + H(0.25 - |x_2|))$, $\varepsilon = 0.025$, where H is the Heaviside step function.

This is consistent with the idea that inhibitory neurons play an important role in shaping the receptive fields of neurons in the visual cortex and that the interaction between excitatory and inhibitory neurons is crucial for visual processing. This new approach offers the advantage of accommodating any geometrical visual stimulus, particularly those localized in the visual field.

We hope that this take on the question can serve as a foundation for future investigations, such as the theoretical replication of other psychophysical phenomena, including Billock and Tsou experiments [3], the apparent motion in quartet stimulus [11], the flickering wheel illusion [24], the spin in the enigma stimulus of Isia Léviant [33, 16], or other psychophysical phenomena involving spontaneous cortical patterns such as the Barber pole, Café wall, Fraser spiral illusions [10, 14], etc..

Appendix A. Equivariance of the input-output map with respect to the plane Euclidean group

We discuss in this section the equivariance of the input to stationary output map Ψ defined in (24) with respect to the plane Euclidean group.

Let $\mathbf{E}(2)$ denote the Euclidean group, which is the symmetry group of $\mathbb{R}^2$. It is well known that (see, [31, Chapter IV] for instance) $\mathbf{E}(2)$ is the cross product of two-dimensional real line space $\mathbb{R}^2$ and $\mathcal{O}(2)$ the group of Euclidean rotations and reflections of this space, the so-called orthogonal group : $\mathbf{E}(2) = \mathbb{R}^2 \rtimes \mathcal{O}(2)$. For any $g = (a, r) \in \mathbf{E}(2)$, one has $(a, r) \in \mathbb{R}^2 \times \mathcal{O}(2)$ and the group property is the following

$$\begin{cases} g_1 \cdot g_2 = (a_1, r_1) \cdot (a_2, r_2) = (r_1 a_2 + a_1, r_1 r_2), \\ g^{-1} = (-r^{-1} a, r^{-1}), \\ e = (0, \mathrm{Id}). \end{cases}$$

Here, g^{-1} is the inverse of $g = (a, r) \in \mathbf{E}(2)$, e is the identity in $\mathbf{E}(2)$ and Id is the identity in $\mathcal{O}(2)$.

Definition A.1 (Action of $\mathbf{E}(2)$ on $\mathbb{R}^2$)**.** *For $x \in \mathbb{R}^2$, the action of $g = (a, r) \in \mathbf{E}(2)$ on $\mathbb{R}^2$ is defined by $gx = rx + a$.*

Definition A.2 (Action of $\mathbf{E}(2)$ on $L^p(\mathbb{R}^2)$)**.** *We define the action of $\mathbf{E}(2)$ on $L^p(\mathbb{R}^2)$ by the representation $T : g \in \mathbf{E}(2) \longmapsto T_g \in \mathrm{GL}(L^p(\mathbb{R}^2))$ such that, for all $v \in L^p(\mathbb{R}^2)$, it holds*

$$(T_g v)(x) = v(g^{-1} x), \qquad x \in \mathbb{R}^2.$$

Here $\mathrm{GL}(L^p(\mathbb{R}^2))$ is the group of automorphism from $L^p(\mathbb{R}^2)$ to itself.

We emphasise that the validity of the following proposition depends solely on the symmetry properties satisfied by the kernel ω rather than the nonlinear function f. It remains valid whatever the shape (even linear, etc.) of the response function f.

Proposition A.3. *Let μ_0 be defined by (11). If $\mu < \mu_0$, then, the map Ψ defined in (24) and its inverse Ψ^{-1} are $\mathbf{E}(2)$-equivariant, that is*

$$\Psi T_g = T_g \Psi \qquad \text{and} \qquad \Psi^{-1} T_g = T_g \Psi^{-1}, \qquad \text{for any } g \in \mathbf{E}(2). \tag{74}$$

Remark A.4. *As a consequence of Proposition A.3 we have that the sensory input I and the stationary output $\Psi(I)$ have the same symmetry subgroups $\Gamma \subset \mathbf{E}(2)$. For example, I depends solely on the x_1 variable if and only if the same is true for $\Psi(I)$.*

Proof of Proposition A.3. We start by claiming that $\mathcal{Q}(v) := \omega * f(v)$ is an $\mathbf{E}(2)$-equivariant operator from $L^p(\mathbb{R}^2)$ to itself. The fact that $\mathcal{Q}$ is well-defined is a consequence of Lemma 3.2. We thus need to show that $T_g \mathcal{Q} = \mathcal{Q} T_g$, for any $g = (a, r) \in \mathbf{E}(2)$. Let $v \in L^p(\mathbb{R}^2)$ and $x \in \mathbb{R}^2$. On one hand, one has

$$(T_g(\mathcal{Q}(v)))(x) = \mathcal{Q}(v)(g^{-1} x) = \int_{\mathbb{R}^2} \omega(|g^{-1} x - y|) f(v(y)) dy. \tag{75}$$

On the other hand, one has

$$(\mathcal{Q}(T_g v))(x) = \int_{\mathbb{R}^2} \omega(|x-y|)(f(T_g v))(y)dy = \int_{\mathbb{R}^2} \omega(|x-y|)f(v(r^{-1}(y-a)))dy.$$

Setting $z = r^{-1}(y-a)$, then $dy = |\det r|dz = dz$, since $r \in \mathcal{O}(2)$ and

$$|x - rz - a| = |r(r^{-1}(x-a) - z)| = |g^{-1}x - z|.$$

It follows that

$$(\mathcal{Q}(T_g v))(x) = \int_{\mathbb{R}^2} \omega(|g^{-1}x - z|)f(v(z))dz, \tag{76}$$

which completes the proof of the claim by identifying (75) and (76).

To complete the proof of the statement, we need to show that $T_g\Psi = \Psi T_g$ and $T_g\Psi^{-1} = \Psi^{-1}T_g$ for any $g \in \mathbf{E}(2)$. This is equivalent to prove that for all $I \in L^p(\mathbb{R}^2)$, $T_g\Psi(I) = \Psi(T_g I)$ and $T_g\Psi^{-1}(I) = \Psi^{-1}(T_g I)$. It follows from the previous claim that

$$T_g\Psi(I) = T_g I + \mu T_g\mathcal{Q}(\Psi(I)) = T_g I + \mu\mathcal{Q}(T_g\Psi(I)).$$

On the other hand, one has

$$\Psi(T_g I) = T_g I + \mu\mathcal{Q}(\Psi(T_g I)).$$

So, by the uniqueness of the stationary state provided by Theorem 3.3, we obtain $T_g\Psi(I) = \Psi(T_g I)$. Arguing similarly, we prove that Ψ^{-1} is also $\mathbf{E}(2)$-equivariant. □

Appendix B. Complement results

B.1. **Complement results for the MacKay effect replication in the linear regime.** This section contains various complements used in Section 5.2 to describe the MacKay effect when the response function in Equation (NF) is linear. The first result is the following.

Theorem B.1. *Under the considerations of Remark 5.10, the kernel K defined in (59) can be recast for all $x \in \mathbb{R}^*$ as*

$$\begin{aligned}\frac{K(x)}{2\sqrt{\pi}} &= e^{-\pi|x|\sqrt{\frac{2\pi}{3}}}\cos\left(\frac{\pi}{12} + \pi|x|\sqrt{\frac{2\pi}{3}}\right) + \sum_{k=1}^{\infty}\frac{e^{-\pi c_k|x|\sqrt{\frac{2\pi}{3}}}}{c_k}\cos\left(\frac{\pi}{12} + \pi c_k|x|\sqrt{\frac{2\pi}{3}}\right)\\ &\quad + \sum_{k=1}^{\infty}\frac{e^{-\pi d_k|x|\sqrt{\frac{2\pi}{3}}}}{d_k}\sin\left(\frac{\pi}{12} - \pi d_k|x|\sqrt{\frac{2\pi}{3}}\right),\end{aligned} \tag{77}$$

where

$$c_k = \sqrt{1+6k} \qquad k \in \mathbb{N} \qquad \text{and} \qquad d_k = \sqrt{-1+6k}, \qquad k \in \mathbb{N}^*. \tag{78}$$

Proof. We start by introducing for a fixed $x \in \mathbb{R}$, the function

$$g : z \in \mathbb{C} \mapsto g(z) = e^{2i\pi zx}\frac{\widehat{\omega_1}(z)}{1-\widehat{\omega_1}(z)} = e^{2i\pi zx}\widehat{K}(z), \qquad \widehat{\omega_1}(z) = e^{-z^2} - e^{-2z^2}. \tag{79}$$

We have that g is a meromorphic function with simple poles (zeroes of the exponential polynomial h defined in (61)) distributed as in Figure 9 that we enumerate as $p_{k,\ell}$ and $q_{k,\ell}$ where $\ell \in \{0, \cdots, 3\}$, by

$$p_{k,\ell} = c_k e^{i\frac{\pi}{4}}i^\ell\sqrt{\frac{\pi}{3}}, \qquad k \in \mathbb{N} \qquad \text{and} \qquad q_{k,\ell} = d_k e^{i\frac{\pi}{4}}i^\ell\sqrt{\frac{\pi}{3}}, \qquad k \in \mathbb{N}^*, \tag{80}$$

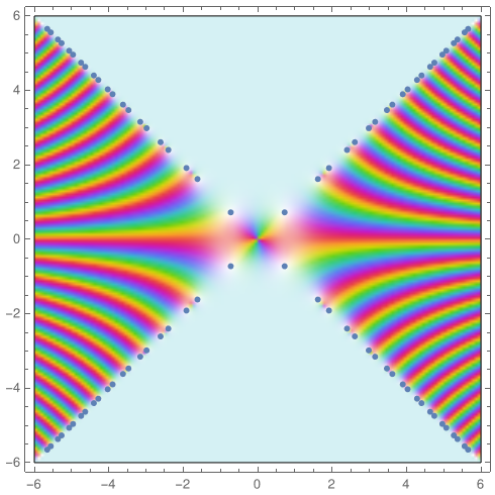

FIGURE 9. Zeroes in the complex plane of the exponential polynomial h defined in (61). Here $\kappa = \mu = 1$, $2\pi^2\sigma_1^2 = 1$ and $2\pi^2\sigma_2^2 = 2$.

where c_k and d_k are defined as in (78). Since $\widehat{\omega}(p_{k,\ell}) = 1 = \widehat{\omega}(q_{k,\ell})$, we find the residues of g to be given by

$$\operatorname{Res}(g, p_{k,\ell}) = -\frac{e^{i\frac{\pi}{4}} i^\ell e^{i(-1)^\ell \frac{\pi}{3}}}{2c_k\sqrt{\pi}} e^{2i\pi x p_{k,\ell}}, \qquad k \in \mathbb{N}, \tag{81}$$

$$\operatorname{Res}(g, q_{k,\ell}) = \frac{e^{i\frac{\pi}{4}} i^\ell e^{-i(-1)^\ell \frac{\pi}{3}}}{2d_k\sqrt{\pi}} e^{2i\pi x q_{k,\ell}}, \qquad k \in \mathbb{N}^*. \tag{82}$$

We now fix $x > 0$, and we let

$$R_n := \sqrt{n\pi}, \qquad n \in \mathbb{N}^*.$$

We consider the path Γ_n straight along the real line axis from $-R_n$ to R_n and then counterclockwise along a semicircle centred at $z = 0$ in the upper half of the complex plane, $\Gamma_n = [-R_n, R_n] \cup C_n^+$, where $C_n^+ = \{R_n e^{i\phi} \mid \phi \in [0, \pi]\}$. Then, by the residue Theorem, one has for all $n \in \mathbb{N}^*$,

$$\begin{aligned}
\int_{-R_n}^{R_n} g(\xi)d\xi + \int_{C_n^+} g(z)dz &= 2\pi i \sum_{\ell=0}^{\ell=1}\sum_{k=0}^{n-1} \operatorname{Res}(g, p_{k,\ell}) + 2\pi i \sum_{\ell=0}^{\ell=1}\sum_{k=1}^{n-1} \operatorname{Res}(g, q_{k,\ell}) \\
&= 2\sqrt{\pi} e^{-\pi x\sqrt{\frac{2\pi}{3}}} \cos\left(\frac{\pi}{12} + \pi x\sqrt{\frac{2\pi}{3}}\right) + \\
&\quad 2\sqrt{\pi}\sum_{k=1}^{n-1} \frac{e^{-\pi c_k x\sqrt{\frac{2\pi}{3}}}}{c_k} \cos\left(\frac{\pi}{12} + \pi c_k x\sqrt{\frac{2\pi}{3}}\right) + \\
&\quad 2\sqrt{\pi}\sum_{k=1}^{n-1} \frac{e^{-\pi d_k x\sqrt{\frac{2\pi}{3}}}}{d_k} \sin\left(\frac{\pi}{12} - \pi d_k x\sqrt{\frac{2\pi}{3}}\right).
\end{aligned} \tag{83}$$

We set

$$A_n(x) := \int_{C_n^+} g(z)dz.$$

Then, one obtains,

$$\begin{aligned} |A_n(x)| &\leq R_n \int_0^{\pi} e^{-2R_n\pi x\sin(\phi)}|\widehat{K}(R_ne^{i\phi})|d\phi \\ &= \underbrace{R_n \int_0^{\frac{\pi}{4}} e^{-2R_n\pi x\sin(\phi)}|\widehat{K}(R_ne^{i\phi})|d\phi}_{J_1} + \underbrace{R_n \int_{\frac{\pi}{4}}^{\frac{3\pi}{4}} e^{-2R_n\pi x\sin(\phi)}|\widehat{K}(R_ne^{i\phi})|d\phi}_{J_2} \\ &\quad + \underbrace{R_n \int_{\frac{3\pi}{4}}^{\pi} e^{-2R_n\pi x\sin(\phi)}|\widehat{K}(R_ne^{i\phi})|d\phi}_{J_3}. \end{aligned} \tag{84}$$

Since $|\widehat{K}(R_ne^{i\phi})| \leq 1$ for all $\phi \in [0,\pi]$, uniformly w.r.t. $n \in \mathbb{N}^*$, one has for all $x > 0$,

$$\begin{aligned} J_2 := R_n \int_{\frac{\pi}{4}}^{\frac{3\pi}{4}} e^{-2R_n\pi x\sin(\phi)}|\widehat{K}(R_ne^{i\phi})|d\phi &\leq R_n \int_{\frac{\pi}{4}}^{\frac{3\pi}{4}} e^{-2R_n\pi x\sin(\phi)}d\phi \\ &\leq \frac{\pi R_n}{2} e^{-R_n\pi x\sqrt{2}} \xrightarrow[n\to+\infty]{} 0. \end{aligned} \tag{85}$$

On the other hand, there exist a positive constant $C > 0$ independent of $n \in \mathbb{N}^*$ ($C := 3/2$ is valid) such that for all $\phi \in [0,\pi]$, it holds

$$|\widehat{K}(R_ne^{i\phi})| = \left|\frac{\widehat{\omega_1}(R_ne^{i\phi})}{1-\widehat{\omega_1}(R_ne^{i\phi})}\right| \leq C|\widehat{\omega_1}(R_ne^{i\phi})| \leq C\left(e^{-R_n^2\cos(2\phi)} + e^{-2R_n^2\cos(2\phi)}\right), \qquad \forall n \in \mathbb{N}^*.$$

Since $\cos(2\phi) \geq -\frac{4}{\pi}\phi + 1$ for all $\phi \in [0,\pi/4]$, one deduces

$$\begin{aligned} J_1 + J_3 &\leq 2R_n \int_0^{\frac{\pi}{4}} e^{-2R_n\pi x\sin(\phi)}|\widehat{K}(R_ne^{i\phi})|d\phi \leq 2CR_n \int_0^{\frac{\pi}{4}} e^{-R_n^2\cos(2\phi)}d\phi \\ &\leq 4CR_ne^{-R_n^2} \int_0^{\frac{\pi}{4}} e^{\frac{4}{\pi}R_n^2\phi}d\phi = \frac{C\pi}{R_n}\left[1-e^{-R_n^2}\right] \xrightarrow[n\to+\infty]{} 0. \end{aligned} \tag{86}$$

To summarise, one has for all $x > 0$,

$$\int_{C_n^+} g(z)dz \xrightarrow[n\to+\infty]{} 0.$$

By taking the limit as $n \to +\infty$ in (83) we find for all $x > 0$,

$$\begin{aligned} \frac{K(x)}{2\sqrt{\pi}} &= e^{-\pi x\sqrt{\frac{2\pi}{3}}}\cos\left(\frac{\pi}{12} + \pi x\sqrt{\frac{2\pi}{3}}\right) + \sum_{k=1}^{+\infty} \frac{e^{-\pi c_k x\sqrt{\frac{2\pi}{3}}}}{c_k}\cos\left(\frac{\pi}{12} + \pi c_k x\sqrt{\frac{2\pi}{3}}\right) \\ &\quad + \sum_{k=1}^{+\infty} \frac{e^{-\pi d_k x\sqrt{\frac{2\pi}{3}}}}{d_k}\sin\left(\frac{\pi}{12} - \pi d_k x\sqrt{\frac{2\pi}{3}}\right). \end{aligned} \tag{87}$$

Finally, the result follows at once since K is an even function. □

Remark B.2. *Since the kernel K is even on $\mathbb{R}$, we will restrict its study to $\mathbb{R}_+$.*

In what follows, we aim to prove that K admits a discrete and countable set of zeroes on $\mathbb{R}_+^*$. It is a consequence of the following.

Lemma B.3. *For all $x \in \mathbb{R}_+^*$, it holds that*

$$\frac{e^{\pi x\sqrt{\frac{2\pi}{3}}}K(x)}{2\sqrt{\pi}} = \cos\left(\frac{\pi}{12} + \pi x\sqrt{\frac{2\pi}{3}}\right) + \frac{S(x)}{x}, \tag{88}$$

where

$$|S(x)| \leq \frac{\sqrt{6}}{3\pi^2}. \tag{89}$$

Moreover, the derivative of K satisfies

$$\frac{\sqrt{3}e^{\pi x\sqrt{\frac{2\pi}{3}}}K'(x)}{4\pi^2} = -\sin\left(\frac{\pi}{3} + \pi x\sqrt{\frac{2\pi}{3}}\right) + T(x), \tag{90}$$

where

$$|T(x)| \leq \frac{1 + \pi x\sqrt{\frac{2\pi}{3}}}{\pi^3 x^2}. \tag{91}$$

Proof. Let $x > 0$, one starts with the equation

$$\frac{K(x)}{2\sqrt{\pi}} = e^{-\pi x\sqrt{\frac{2\pi}{3}}}\cos\left(\frac{\pi}{12} + \pi x\sqrt{\frac{2\pi}{3}}\right) + R_1(x) + R_2(x),$$

where $R_1(x) = \sum_{k=1}^{+\infty} r_1(k)\cos\left(\frac{\pi}{12} + \pi c_k x\sqrt{\frac{2\pi}{3}}\right)$ and $R_2(x) = \sum_{k=1}^{+\infty} r_2(k)\sin\left(\frac{\pi}{12} - \pi d_k x\sqrt{\frac{2\pi}{3}}\right)$. The functions r_1 and r_2 are defined on $\mathbb{R}_+$ and $[1/3, +\infty)$ respectively by

$$r_1(t) = \frac{e^{-A\sqrt{1+6t}}}{\sqrt{1+6t}}, \qquad r_2(t) = \frac{e^{-A\sqrt{-1+6t}}}{\sqrt{-1+6t}} \qquad \text{with} \qquad A = \pi x\sqrt{\frac{2\pi}{3}}.$$

Since r_1 is decreasing on $\mathbb{R}_+$ one deduces that

$$|R_1(x)| \leq \sum_{k=1}^{+\infty} r_1(k) \leq \sum_{k=1}^{+\infty}\int_{k-1}^{k} r_1(t)\,dt = \int_0^{\infty} r_1(t)\,dt = \int_0^{\infty} e^{-A\sqrt{1+6t}}\frac{dt}{\sqrt{1+6t}} = \frac{e^{-A}}{3A}.$$

The same argument gives the same inequality for $|R_2(x)|$ and inequality (89) follows at once. On the other hand, it is straightforward to observe that the sum $S(x)$ in (88) is uniformly (normally in fact) convergent on $(-\infty, -B]\cup[B, +\infty)$ for all $B > 0$. Thus, after derivation under the sum, one finds for all $x > 0$,

$$\begin{aligned}
\frac{\sqrt{3}e^{\pi x\sqrt{\frac{2\pi}{3}}}K'(x)}{4\pi^2} &= -\sin\left(\frac{\pi}{3} + \pi x\sqrt{\frac{2\pi}{3}}\right) - e^{\pi x\sqrt{\frac{2\pi}{3}}}\sum_{k=1}^{\infty} e^{-\pi c_k x\sqrt{\frac{2\pi}{3}}}\sin\left(\frac{\pi}{3} + \pi c_k x\sqrt{\frac{2\pi}{3}}\right) \\
&\quad - e^{\pi x\sqrt{\frac{2\pi}{3}}}\sum_{k=1}^{\infty} e^{-\pi d_k x\sqrt{\frac{2\pi}{3}}}\sin\left(\frac{\pi}{3} - \pi d_k x\sqrt{\frac{2\pi}{3}}\right) \\
&= -\sin\left(\frac{\pi}{3} + \pi x\sqrt{\frac{2\pi}{3}}\right) + T(x),
\end{aligned}$$

where

$$|T(x)| \leq e^{\pi x\sqrt{\frac{2\pi}{3}}} \sum_{k=1}^{\infty} \left(e^{-\pi c_k x\sqrt{\frac{2\pi}{3}}} + e^{-\pi d_k x\sqrt{\frac{2\pi}{3}}} \right) \leq 2e^{\pi x\sqrt{\frac{2\pi}{3}}} \sum_{k=1}^{\infty} e^{-\pi d_k x\sqrt{\frac{2\pi}{3}}},$$

since $c_k \geq d_k$ for all $k \geq 1$. But one has

$$\sum_{k=1}^{\infty} e^{-\pi d_k x\sqrt{\frac{2\pi}{3}}} \leq \sum_{k=1}^{\infty} \int_{k-\frac{2}{3}}^{k} e^{-\pi x\sqrt{-1+6t}\sqrt{\frac{2\pi}{3}}} dt = \int_{\frac{1}{3}}^{\infty} e^{-\pi x\sqrt{-1+6t}\sqrt{\frac{2\pi}{3}}} dt = \frac{1+\pi x\sqrt{\frac{2\pi}{3}}}{2\pi^3 x^2} e^{-\pi x\sqrt{\frac{2\pi}{3}}},$$

so that inequality (91) follows at once and completes the proof of the lemma. □

Proposition B.4. *Let $(x_k)_{k\in\mathbb{N}^*}$ and $(y_k)_{k\in\mathbb{N}^*}$ denote the sequences of zeroes and extrema of the function $x \mapsto \cos(\pi/12 + \pi x\sqrt{2\pi/3})$ on $\mathbb{R}_+^*$ respectively. There exists $(z_k)_{k\in\mathbb{N}^*}$, sequence of zeroes of K in $\mathbb{R}_+^*$ such that z_k is the unique zero of K in the interval $I_k :=]y_k, y_{k+1}[$ for all $k \in \mathbb{N}^*$ and*

$$|x_{k+1} - z_k| \leq \frac{\sqrt{3}}{\pi\sqrt{2\pi}} \arcsin\left(\frac{8}{\pi(12k-1)}\right), \qquad \forall k \in \mathbb{N}^*. \tag{92}$$

Proof. We fix $k \in \mathbb{N}^*$, then one has

$$|S(y_k)| \leq \frac{2}{\pi\sqrt{6\pi}y_k} = \frac{8}{\pi(12k-1)} \leq \frac{8}{11\pi} < 1,$$

by Lemma B.3. One deduces that

$$e^{\pi y_k\sqrt{\frac{2\pi}{3}}} \frac{K(y_k)}{2\sqrt{\pi}} = (-1)^k + S(y_k) \begin{cases} < 0, & \text{if} \quad k \quad \text{is odd,} \\ > 0, & \text{if} \quad k \quad \text{is even.} \end{cases}$$

It follows that K admits at least one zero z_k in the interval I_k by the intermediate value theorem. Let us prove that z_k is the unique zero in this interval. We let $\widetilde{z}$ be an arbitrary zero of K in the interval I_k and set $e_k := \widetilde{z} - x_{k+1}$. Then one has by Lemma B.3

$$S(\widetilde{z}) = -\cos\left(\frac{\pi}{12} + \pi\widetilde{z}\sqrt{\frac{2\pi}{3}}\right) = (-1)^k \sin\left(\pi e_k\sqrt{\frac{2\pi}{3}}\right), \tag{93}$$

and

$$\left|\sin\left(\pi e_k\sqrt{\frac{2\pi}{3}}\right)\right| \leq \frac{2}{\pi\sqrt{6\pi\widetilde{z}}} \leq \frac{2}{\pi\sqrt{6\pi}y_k} \leq \frac{2}{\pi\sqrt{6\pi}y_1} = \frac{8}{11\pi}. \tag{94}$$

On the other hand, using (93) and trigonometric identity for sine, one obtains

$$\begin{aligned} \frac{\sqrt{3}e^{\pi\widetilde{z}\sqrt{\frac{2\pi}{3}}}K'(\widetilde{z})}{4\pi^2} &= -\sin\left(\frac{\pi}{12} + \pi\widetilde{z}\sqrt{\frac{2\pi}{3}} + \frac{\pi}{4}\right) + T(\widetilde{z}) \\ &= \frac{(-1)^{k+1}}{\sqrt{2}} \cos\left(\pi e_k\sqrt{\frac{2\pi}{3}}\right) + \frac{1}{\sqrt{2}}S(\widetilde{z}) + T(\widetilde{z}). \end{aligned} \tag{95}$$

By using (93), (94) and (91) one finds

$$\cos\left(\pi e_k\sqrt{\frac{2\pi}{3}}\right) \geq \sqrt{1-\frac{8}{11\pi}} > \sqrt{1-\frac{1}{2}} = \frac{1}{\sqrt{2}},$$

and

$$\left|\frac{1}{\sqrt{2}}S(\widetilde{z})+T(\widetilde{z})\right| \leq \frac{1}{\sqrt{2}}\frac{8}{11\pi}+\frac{1+\pi y_1\sqrt{\frac{2\pi}{3}}}{\pi^3 y_1^2} < \frac{1}{2}.$$

It follows that

$$K'(\widetilde{z}) \begin{cases} > 0, & \text{if} \quad k \quad \text{is odd,} \\ < 0, & \text{if} \quad k \quad \text{is even.} \end{cases}$$

Let $\widetilde{z}$ and $\widetilde{z}'$ be successive zeroes of K in I_k and assume that k is odd to be fixed. Then $K'(\widetilde{z}) > 0$ and $K'(\widetilde{z}') > 0$. By Rolle's theorem, there exists $\widetilde{z}'' \in (\widetilde{z}, \widetilde{z}')$ such that $K(\widetilde{z}'') = 0$ and $K'(\widetilde{z}'') < 0$, which is a contradiction of the fact that any zero $\widetilde{z}$ in I_k satisfies $K'(\widetilde{z}) > 0$. Thus, z_k is the unique zero of K in the interval I_k. Finally, inequality (94) applied with $\widetilde{z} = z_k$ leads to inequality (92), and this completes the proof of the proposition. □

Remark B.5. *Suppose we model the interaction of V1 neurons in Equation (NF) with a Gaussian kernel ω. In that case, we will obtain that the associated kernel $\widehat{K}$ defined in (79) has two isolated poles located on the imaginary axis of the complex plane. The zero-order terms which dominate the expansion of K given by (77) are only an exponential decreasing function without a cosine multiplicative factor. Therefore, the kernel K will never have infinitely many discrete distributed zeroes.*

B.2. **Miscellaneous complements.** Some of the results provided in this section were used in Section 5.3 to describe the MacKay effect when the response function in Equation (NF) is nonlinear.

We recall from Theorem 3.3 that, given $1 \leq p \leq \infty$ and $I \in L^p(\mathbb{R}^2)$, then for any $a_0 \in L^p(\mathbb{R}^2)$, the initial value Cauchy problem associated with Equation (NF) has a unique solution $a \in X_p$. It is implicitly given for all $x \in \mathbb{R}^2$, and every $t \geq 0$ by

$$a(x,t) = e^{-t}a_0(x) + \left(1-e^{-t}\right) I(x) + \mu \int_0^t e^{-(t-s)}(\omega * f(a))(x,s)ds. \tag{96}$$

Given $I \in L^\infty(\mathbb{R}^2)$, the following theorem improves the upper bound of the L^∞-norm of the stationary state $a_I \in L^\infty(\mathbb{R}^2)$ provided in (25).

Theorem B.6. *Let $a_0 \in L^\infty(\mathbb{R}^2)$, $I \in L^\infty(\mathbb{R}^2)$ with $\|I\|_\infty = 1$ and $a \in X_\infty$ be the solution of (NF). It holds*

$$\limsup_{t\to+\infty} \|a(\cdot,t)\|_\infty \leq g_1, \tag{97}$$

where $g_1 > 0$ is the smaller fixed point of the following function

$$g : x \in \mathbb{R} \longmapsto 1 + \frac{\mu}{\mu_0} f(x) \in \mathbb{R}_+^*. \tag{98}$$

Proof. We start by using (96), (14) and Minkowski's inequality to obtain for a.e. $x \in \mathbb{R}^2$ and every $t \geq 0$,

$$|a(x,t)| \leq e^{-t}\|a_0\|_{L^\infty} + (1-e^{-t}) + \frac{\mu}{\mu_0}(1-e^{-t}). \tag{99}$$

Letting $t \to \infty$ in the last inequality, we find $V_\infty := \limsup_{t\to+\infty} \|a(\cdot,t)\|_\infty \leq 1 + \mu/\mu_0$, showing in particular that $V_\infty < \infty$. It follows that

$$\forall \varepsilon > 0,\ \exists T_\varepsilon > 0 \text{ s.t., } \forall t \geq T_\varepsilon,\ \ \|a(\cdot,t)\|_\infty \leq V_\infty + \varepsilon. \tag{100}$$

Applying the variation of constants formula (96), starting at $T_\varepsilon > 0$, one deduces for every $t > T_\varepsilon$ that

$$\begin{aligned} \|a(\cdot,t)\|_\infty &\leq e^{-(t-T_\varepsilon)}\|a(\cdot,T_\varepsilon)\|_\infty + \left(1-e^{-(t-T_\varepsilon)}\right) + \mu\|\omega\|_1 \int_{T_\varepsilon}^t e^{-(t-s)} f(\|a(\cdot,s)\|_\infty) ds \\ &\leq e^{-(t-T_\varepsilon)}(V_\infty+\varepsilon) + 1 + \frac{\mu}{\mu_0} f(V_\infty+\varepsilon). \end{aligned} \tag{101}$$

Letting respectively $t \to \infty$ and $\varepsilon \to 0$ in the preceding inequality we find

$$V_\infty \leq 1 + \frac{\mu}{\mu_0} f(V_\infty). \tag{102}$$

Let $(u_n)_n$ be the real sequence defined by

$$u_0 = V_\infty, \qquad u_{n+1} = g(u_n), \qquad \forall n \geq 1. \tag{103}$$

Then $(u_n)_n$ is a bounded and non-decreasing sequence. The boundedness of $(u_n)_n$ follows from the boundedness[4] of the sigmoid function f. Let us prove by induction that the sequence $(u_n)_n$ is increasing. Due to the inequality (102), one has

$$u_1 = g(u_0) = 1 + \frac{\mu}{\mu_0} f(u_0) = 1 + \frac{\mu}{\mu_0} f(V_\infty) \geq V_\infty = u_0.$$

If $u_n \geq u_{n-1}$ then, since f is non-decreasing, one obtains

$$u_{n+1} = g(u_n) = 1 + \frac{\mu}{\mu_0} f(u_n) \geq 1 + \frac{\mu}{\mu_0} f(u_{n-1}) = g(u_{n-1}) = u_n,$$

showing that $(u_n)_n$ is a non-decreasing sequence. The monotone convergence and fixed point Theorems, we have that $(u_n)_n$ converges to the smaller fixed point $g_1 > 0$ of the function g, and (97) follows. □

Let $1 \leq p \leq \infty$, we introduce for every $I \in L^p(\mathbb{R}^2)$, the map $\Phi_I : L^p(\mathbb{R}^2) \mapsto L^p(\mathbb{R}^2)$ defined for all $v \in L^p(\mathbb{R}^2)$ by

$$\Phi_I(v) = I + \mu\omega * f(v). \tag{104}$$

Theorem B.7. *Let $1 < p \leq \infty$. If $\mu < \mu_0$, then Ψ belongs to $C^1(L^p(\mathbb{R}^2); L^p(\mathbb{R}^2))$ and the differential at $I \in L^p(\mathbb{R}^2)$ is given by*

$$D\Psi(I)h = (\mathrm{Id} - D\Psi(I))^{-1}h, \qquad \forall h \in L^p(\mathbb{R}^2). \tag{105}$$

The proof of Theorem B.7 is a consequence of the following two lemmas.

Lemma B.8. *Let $1 < p \leq \infty$, and $I \in L^p(\mathbb{R}^2)$. Then for every $\mu > 0$, the map Φ_I belongs to the space $C^1(L^p(\mathbb{R}^2); L^p(\mathbb{R}^2))$ and the differential at $v \in L^p(\mathbb{R}^2)$ is given by*

$$(D\Phi_I(v)h)(x) = \mu \int_{\mathbb{R}^2} \omega(x-y) f'(v(y)) h(y) dy, \qquad \forall h \in L^p(\mathbb{R}^2),\ x \in \mathbb{R}^2. \tag{106}$$

Moreover, it holds

$$\|D\Phi_I(v)\|_{\mathscr{L}(L^p(\mathbb{R}^2))} \leq \frac{\mu}{\mu_0}, \qquad \forall v \in L^p(\mathbb{R}^2). \tag{107}$$

[4]Notice that in the case where the response function f is only Lipschitz continuous (with the Lipschitz constant equal to $f'(0) = 1$) but not bounded, the sequence $(u_n)_n$ is still bounded, via

$$|u_n| \leq V_\infty + \frac{\mu_0}{\mu_0 - \mu}, \qquad \forall n \in \mathbb{N}.$$

Proof. It is straightforward to show that for all $1 \leq p \leq \infty$, and $I \in L^p(\mathbb{R}^2)$, the map Φ_I is Gateau-differentiable at every $v \in L^p(\mathbb{R}^2)$, the Gateau-differential is given for every $h \in L^p(\mathbb{R}^2)$ by (106). Since f' is bounded by 1, we find

$$\|D\Phi_I(v)h\|_p \leq \frac{\mu}{\mu_0}\|h\|_p. \tag{108}$$

Let us now show that for all $1 < p \leq \infty$, the Gateau-differential

$$\begin{aligned} D\Phi_I : \quad L^p(\mathbb{R}^2) &\longrightarrow \mathscr{L}(L^p(\mathbb{R}^2)) \\ v &\longmapsto D\Phi_I(v), \end{aligned} \tag{109}$$

is continuous. To this end, let $(v_n) \subset L^p(\mathbb{R}^2)$ be a real sequence converging in the L^p-norm to $v \in L^p(\mathbb{R}^2)$. We want to prove that $D\Phi_I(v_n)$ converges to $D\Phi_I(v)$ in $\mathscr{L}(L^p(\mathbb{R}^2))$. Let $h \in L^p(\mathbb{R}^2)$ and set

$$R_n : x \in \mathbb{R}^2 \longmapsto R_n(x) = \int_{\mathbb{R}^2} \omega(x-y)[f'(v_n(y)) - f'(v(y))]h(y)dy. \tag{110}$$

It is immediate to obtain the result when $p = \infty$. Indeed, since f' is $\|f''\|_\infty$-Lipschitz continuous, one immediately gets that

$$\|R_n\|_\infty \leq \|f''\|_\infty \|\omega\|_1 \|v_n - v\|_\infty \|h\|_\infty,$$

so that

$$\begin{aligned} \|D\Phi_I(v_n) - D\Phi_I(v)\|_{\mathscr{L}(L^\infty(\mathbb{R}^2))} &= \sup_{\substack{h \in L^\infty(\mathbb{R}^2) \\ \|h\|_\infty = 1}} \|D\Phi_I(v_n)h - D\Phi_I(v)h\|_\infty \\ &\leq \mu\|f''\|_\infty\|\omega\|_1\|v_n - v\|_\infty \xrightarrow[n\to\infty]{} 0. \end{aligned} \tag{111}$$

Let us turn to an argument for the cases $1 < p < \infty$. Since (v_n) tends in the L^p-norm to $v \in L^p(\mathbb{R}^2)$, for every $\varepsilon > 0$, there exists a positive integer $N \in \mathbb{N}$ such that for any $n \geq N$ it holds $\|v_n - v\|_p \leq \varepsilon$. In the following, we fix $\varepsilon > 0$ and N defined previously. For every $n \in \mathbb{N}$ such that $n \geq N$, we consider $E_n := \{y \in \mathbb{R}^2 \mid |v_n(y) - v(y)| > \sqrt{\varepsilon}\}$, one has for every $x \in \mathbb{R}^2$,

$$R_n(x) = \underbrace{\int_{\mathbb{R}^2 \setminus E_n} \omega(x-y)[f'(v_n(y)) - f'(v(y))]h(y)dy}_{\Lambda_1(x)} + \underbrace{\int_{E_n} \omega(x-y)[f'(v_n(y)) - f'(v(y))]h(y)dy}_{\Lambda_2(x)}. \tag{112}$$

By Chebyshev's inequality, it holds that

$$|E_n| \leq \frac{\|v_n - v\|_p^p}{\varepsilon^{\frac{p}{2}}} \leq \varepsilon^{\frac{p}{2}}, \tag{113}$$

where $|E_n|$ denotes the Lebesgue measure of the measurable set $E_n \subset \mathbb{R}^2$.

On one hand, using Hölder inequality and the fact that f' is $\|f''\|_\infty$-Lipschitz continuous, one has

$$|\Lambda_1(x)| \leq \|f''\|_\infty \sqrt{\varepsilon}\|\omega\|_1^{\frac{1}{q}} \left\{ \int_{\mathbb{R}^2 \setminus E_n} |\omega(x-y)||h(y)|^p dy \right\}^{\frac{1}{p}}, \qquad \forall x \in \mathbb{R}^2.$$

Taking the p-th power on both sides of the above inequality and integrating it with variable x over $\mathbb{R}^2$, we find, thanks to Fubini's theorem,

$$\|\Lambda_1\|_p := \left\{ \int_{\mathbb{R}^2} |\Lambda_1(x)|^p dx \right\}^{\frac{1}{p}} \leq \|f''\|_\infty \|\omega\|_1 \sqrt{\varepsilon}\|h\|_p. \tag{114}$$

On the other hand, using Hölder inequality and the fact that f' is bounded by 1, one has

$$|\Lambda_2(x)|^p \leq 2^p |E_n|^{\frac{p}{q}} \int_{E_n} |\omega(x-y)|^p |h(y)|^p dy, \qquad \forall x \in \mathbb{R}^2.$$

Integrating the above inequality with variable x over $\mathbb{R}^2$, we find, thanks to Fubini's theorem,

$$\|\Lambda_2\|_p := \left\{ \int_{\mathbb{R}^2} |\Lambda_2(x)|^p dx \right\}^{\frac{1}{p}} \leq 2|E_n|^{\frac{1}{q}} \|\omega\|_p \|h\|_p \leq 2\|\omega\|_p \|h\|_p (\sqrt{\varepsilon})^{p-1}, \tag{115}$$

where the last inequality is obtained thanks to (113) and $p/q = p-1$.

Taking now the p-th power on both sides of inequality (112), integrating it with variable x over $\mathbb{R}^2$, applying Minkowski's inequality and using (114) and (115), one gets

$$\|R_n\|_p \leq (\|f''\|_\infty \|\omega\|_1 + 2\|\omega\|_p) \max(\sqrt{\varepsilon}, (\sqrt{\varepsilon})^{p-1}) \|h\|_p.$$

Therefore,

$$\begin{aligned} \|D\Phi_I(v_n) - D\Phi_I(v)\|_{\mathscr{L}(L^p(\mathbb{R}^2))} &= \sup_{\substack{h \in L^p(\mathbb{R}^2) \\ \|h\|_p = 1}} \|D\Phi_I(v_n)h - D\Phi_I(v)h\|_p \\ &\leq \mu(\|f''\|_\infty \|\omega\|_1 + 2\|\omega\|_p) \max(\sqrt{\varepsilon}, (\sqrt{\varepsilon})^{p-1}). \end{aligned} \tag{116}$$

Letting ε tend to zero, one deduces that $D\Phi_I$ is continuous. Finally, using (108) we find for all $v \in L^p(\mathbb{R}^2)$,

$$\|D\Phi_I(v)\|_{\mathscr{L}(L^p(\mathbb{R}^2))} = \sup_{\substack{h \in L^p(\mathbb{R}^2) \\ \|h\|_p = 1}} \|D\Phi_I(v)h\|_p \leq \frac{\mu}{\mu_0},$$

completing the proof of the lemma. □

Lemma B.9. *Let $1 < p \leq \infty$. Under assumption $\mu < \mu_0$, the map*

$$\begin{aligned} \mathcal{G} : \quad L^p(\mathbb{R}^2) \times L^p(\mathbb{R}^2) &\longrightarrow L^p(\mathbb{R}^2) \\ (I, a) &\longmapsto \mathcal{G}(I, \Psi(I)) = a - \Phi_I(a), \end{aligned} \tag{117}$$

belongs to $C^1(L^p(\mathbb{R}^2) \times L^p(\mathbb{R}^2); L^p(\mathbb{R}^2))$ and the partial derivative $D_a\mathcal{G}(I,a)$ is invertible in $\mathscr{L}(L^p(\mathbb{R}^2))$.

Proof. Since Φ_I is differentiable at $a \in L^p(\mathbb{R}^2)$ for all $I \in L^p(\mathbb{R}^2)$, one has for all $(J,b) \in L^p(\mathbb{R}^2) \times L^p(\mathbb{R}^2)$,

$$\begin{aligned} \mathcal{G}(I+J, a+b) &= a + b - \Phi_{I+J}(a) - D\Phi_{I+J}(a)b + o(\|b\|_p) \\ &= \mathcal{G}(I,a) + (\mathrm{Id} - D\Phi_I(a))b - J + o(\|b\|_p). \end{aligned}$$

The map $L_{(I,a)} : L^p(\mathbb{R}^2) \times L^p(\mathbb{R}^2) \longrightarrow L^p(\mathbb{R}^2)$, $L_{(I,a)}(J,b) = (\mathrm{Id} - D\Phi_I(a))b - J$, is linear and bounded,

$$\|L_{(I,a)}(J,b)\|_{L^p(\mathbb{R}^2)} \leq \left(1 + \frac{\mu}{\mu_0}\right) \|(J,b)\|_{L^p(\mathbb{R}^2) \times L^p(\mathbb{R}^2)}.$$

It follows that $\mathcal{G}$ is differentiable at $(I,a) \in L^p(\mathbb{R}^2) \times L^p(\mathbb{R}^2)$ and

$$D\mathcal{G}(I,a)(J,b) = (\mathrm{Id} - D\Phi_I(a))b - J, \qquad \forall (J,b) \in L^p(\mathbb{R}^2) \times L^p(\mathbb{R}^2).$$

We now show that the map $(I,a) \in L^p(\mathbb{R}^2)^2 \mapsto D\mathcal{G}(I,a) \in \mathscr{L}(L^p(\mathbb{R}^2)^2, L^p(\mathbb{R}^2))$ is continuous. Let $(I_1,a_1), (I_2,a_2) \in L^p(\mathbb{R}^2) \times L^p(\mathbb{R}^2)$. One has for all $(J,b) \in L^p(\mathbb{R}^2) \times L^p(\mathbb{R}^2)$,

$$\begin{aligned} \|D\mathcal{G}(I_1,a_1)(J,b) - D\mathcal{G}(I_2,a_2)(J,b)\|_p &= \|D\Phi_{I_1}(a_1)b - D\Phi_{I_2}(a_2)b\|_p \\ &\leq \|D\Phi_{I_1}(a_1) - D\Phi_{I_1}(a_2)\|_{\mathscr{L}(L^p(\mathbb{R}^2))} \|(b,J)\|_{L^p(\mathbb{R}^2)^2}. \end{aligned}$$

It follows by Lemma B.8 that

$$\begin{aligned}\|D\mathcal{G}(I_1,a_1)-D\mathcal{G}(I_2,a_2)\|_{\mathscr{L}(L^p(\mathbb{R}^2)^2,L^p(\mathbb{R}^2))} &\leq \|D\Phi_{I_1}(a_1)-D\Phi_{I_2}(a_2)\|_{\mathscr{L}(L^p(\mathbb{R}^2))}\\ &\leq \mu\|f\|_\infty\|\omega\|_1\|(I_1,a_1)-(I_2,a_2)\|_{L^p(\mathbb{R}^2)^2},\end{aligned}$$

showing that $\mathcal{G}$ belongs to $C^1(L^p(\mathbb{R}^2)\times L^p(\mathbb{R}^2);L^p(\mathbb{R}^2))$. Finally, if $I\in L^p(\mathbb{R}^2)$, $a_I:=\Psi(I)\in L^p(\mathbb{R}^2)$ then $D_a\mathcal{G}(I,a_I)=\mathrm{Id}-D\Phi_I(a_I)$, is invertible in $\mathscr{L}(L^p(\mathbb{R}^2))$ if $\mu<\mu_0$. □

We now can present the proof of Theorem B.7.

Proof of Theorem B.7. Let $\mu<\mu_0$. For fixed $I\in L^p(\mathbb{R}^2)$, $a_I:=\Psi(I)\in L^p(\mathbb{R}^2)$, we have $\mathcal{G}(I,a_I)=0$, and $D_a\mathcal{G}(I,a_I)$ is invertible in $\mathscr{L}(L^p(\mathbb{R}^2))$ by Lemma B.9. It follows by the implicit function Theorem that there is an open neighbourhood $\mathcal{V}$ of I in $L^p(\mathbb{R}^2)$, an open neighbourhood $\mathcal{W}$ of a_I in $L^p(\mathbb{R}^2)$ and a map $\Sigma:\mathcal{V}\to\mathcal{W}$ of class C^1 such that the following holds

$$(I\in\mathcal{V},\ a\in\mathcal{W}\text{ and }\ \mathcal{G}(I,a)=0)\iff(I\in\mathcal{V}\text{ and }\ a=\Sigma(I)).$$

Thereby, $\Psi(\cdot)|_{\mathcal{V}}=\Sigma(\cdot)$ and then Ψ is C^1 at I. Since $I\in L^p(\mathbb{R}^2)$ is arbitrary, it follows that Ψ belongs to $C^1(L^p(\mathbb{R}^2);L^p(\mathbb{R}^2))$. Moreover, taking the derivative of $\mathcal{G}(I,\Psi(I))=0$ at I, one deduces that

$$(\mathrm{Id}-D\Phi_I(\Psi(I)))\,(D\Psi(I)h)=h,\qquad\forall h\in L^p(\mathbb{R}^2). \tag{118}$$

Thus, (105) is an immediate consequence of (107), (118) and the Neumann expansion lemma. □

Lemma B.10. *Let $1<p\leq\infty$, $T>0$ and consider the solution U to (35). Then, $D_{a_0}U(t,v)$ is a well-defined invertible operator for any $v\in L^p(\mathbb{R}^2)$ and every $0\leq t\leq T$. Moreover, it holds*

$$\begin{aligned}\|D_{a_0}U(t,v)-\mathrm{Id}\,\|_{\mathscr{L}(L^p(\mathbb{R}^2))}&\leq t\left(1+\frac{\mu}{\mu_0}\right)e^{\left(1+\frac{\mu}{\mu_0}\right)t},\\ \|\,[D_{a_0}U(t,v)]^{-1}-\mathrm{Id}\,\|_{\mathscr{L}(L^p(\mathbb{R}^2))}&\leq t\left(1+\frac{\mu}{\mu_0}\right)e^{\left(1+\frac{\mu}{\mu_0}\right)t}.\end{aligned} \tag{119}$$

Proof. From Lemma B.8, one gets $DN(U(t,v))=-\mathrm{Id}+D\Phi_0(U(t,v))$. One deduces that for every $\mathrm{V}\in\mathscr{L}(L^p(\mathbb{R}^2))$, it holds

$$\begin{aligned}\|DN(U(t,v))\,\mathrm{V}\,\|_{\mathscr{L}(L^p(\mathbb{R}^2))}&\leq\|DN(U(t,v))\|_{\mathscr{L}(L^p(\mathbb{R}^2))}\|\,\mathrm{V}\,\|_{\mathscr{L}(L^p(\mathbb{R}^2))}\\ &\leq\left(1+\frac{\mu}{\mu_0}\right)\|\,\mathrm{V}\,\|_{\mathscr{L}(L^p(\mathbb{R}^2))}.\end{aligned} \tag{120}$$

It follows that $DN(U(t,v))$ is a bounded linear operator on $\mathscr{L}(L^p(\mathbb{R}^2))$. One also has that $t\in[0,T]\mapsto U(t,v)\in L^p(\mathbb{R}^2)$ is continuous and that $u\in L^p(\mathbb{R}^2)\mapsto D\Phi_0(u)\in\mathscr{L}(L^p(\mathbb{R}^2))$ is continuous thanks to Lemma B.8. Together with (120), one deduces that $t\in[0,T]\mapsto DN(U(t,v))\in\mathscr{L}(\mathscr{L}(L^p(\mathbb{R}^2)))$ is continuous.

By integrating (35), one gets for any $a_0\in L^p(\mathbb{R}^2)$ and $t\geq0$,

$$U(t,a_0)=a_0+\int_0^t N(U(s,a_0))\,ds. \tag{121}$$

It is immediate to see that $U(t,\cdot)$ is differentiable with respect to a_0 for every $t\geq0$ and we use $D_{a_0}U(t,v)$ to denote the evaluation of this differential at any $v\in L^p(\mathbb{R}^2)$. Actually,

differentiating (121) yields that $D_{a_0}U(\cdot,v)$ belongs to $C^1([0,T],\mathscr{L}(L^p(\mathbb{R}^2)))$ for every $T>0$ and satisfies

$$D_{a_0}U(t,v)=\mathrm{Id}+\int_0^t DN(U(s,v))D_{a_0}U(s,v)ds,\qquad 0\le t\le T. \tag{122}$$

Differentiating the above equation, one sees that $t\mapsto DU_{a_0}(t,v)$ is the solution of the homogeneous initial value problem

$$\begin{cases}\partial_t D_{a_0}U(t,v) &= DN(U(t,v))D_{a_0}U(t,v),\\ D_{a_0}U(0,v) &= \mathrm{Id},\end{cases} \tag{123}$$

defined for any $v\in L^p(\mathbb{R}^2)$ and every $0\le t\le T$. This system is nothing else but the differential of (35) with respect to a_0. By [21, Theorem 5.2.-item (i)], one has

$$\|D_{a_0}U(t,v)\|_{\mathscr{L}(L^p(\mathbb{R}^2))}\le e^{\left(1+\frac{\mu}{\mu_0}\right)t},\qquad 0\le t\le T. \tag{124}$$

By combining (122) and (124), one obtains the first inequality in (119). On the other hand, (122) ensures that for $t\in[0,T]$ small enough, $D_{a_0}U(s,v)$ is invertible in $\mathscr{L}(L^p(\mathbb{R}^2))$ for every $s\in[0,t]$ and it holds

$$\begin{cases}\partial_s\left[D_{a_0}U(s,v)\right]^{-1} &= -\left[D_{a_0}U(s,v)\right]^{-1}DN(U(s,v)),\\ \left[D_{a_0}U(0,v)\right]^{-1} &= \mathrm{Id}\,.\end{cases} \tag{125}$$

Arguing as above, one obtains that the homogeneous initial value problem (125) admits a unique solution $\left[D_{a_0}U(\cdot,v)\right]^{-1}\in C^1([0,t],\mathscr{L}(L^p(\mathbb{R}^2)))$ given by

$$\left[D_{a_0}U(s,v)\right]^{-1}=\mathrm{Id}-\int_0^s\left[D_{a_0}U(\tau,v)\right]^{-1}DN(U(\tau,v))d\tau,\qquad 0\le s\le t. \tag{126}$$

Moreover, one has

$$\|\left[D_{a_0}U(s,v)\right]^{-1}\|_{\mathscr{L}(L^p(\mathbb{R}^2))}\le e^{\left(1+\frac{\mu}{\mu_0}\right)s},\qquad 0\le s\le t, \tag{127}$$

and the second inequality in (119) follows for $t\in[0,T]$ small enough. Since (123) holds for every $0\le t\le T$, one can iterate this procedure in $[t,2t],\cdots$, to prove that $D_{a_0}U(t,v)$ is invertible in $\mathscr{L}(L^p(\mathbb{R}^2))$ for every $t\in[0,T]$ and that the second inequality in (119) holds. □

References

[1] S. Amari. "Dynamics of pattern formation in lateral-inhibition type neural fields". In: *Biological cybernetics* 27.2 (1977), pp. 77–87.

[2] C. A. Berenstein and R. Gay. *Complex analysis and special topics in harmonic analysis*. Springer Science & Business Media, 2012.

[3] V. A. Billock and B. H. Tsou. "Neural interactions between flicker-induced self-organized visual hallucinations and physical stimuli". In: *Proceedings of the National Academy of Sciences* 104.20 (2007), pp. 8490–8495. ISSN: 0027-8424. eprint: https://www.pnas.org/content/104/20/8490.full.pdf.

[4] P. C. Bressloff, J. D. Cowan, M. Golubitsky, P. J. Thomas, and M. C. Wiener. "Geometric visual hallucinations, Euclidean symmetry and the functional architecture of striate cortex". In: *Philosophical Transactions of the Royal Society of London. Series B: Biological Sciences* 356.1407 (2001), pp. 299–330.

[5] P. C. Bressloff, J. D. Cowan, M. Golubitsky, P. J. Thomas, and M. C. Wiener. "What geometric visual hallucinations tell us about the visual cortex". In: *Neural computation* 14.3 (2002), pp. 473–491.

[6] L. Brivadis, C. Tamekue, A. Chaillet, and J. Auriol. "Existence of an equilibrium for delayed neural fields under output proportional feedback". In: *Automatica* 151 (2023), p. 110909. ISSN: 0005-1098.

[7] R. Curtu and B. Ermentrout. "Pattern formation in a network of excitatory and inhibitory cells with adaptation". In: *SIAM Journal on Applied Dynamical Systems* 3.3 (2004), pp. 191–231.

[8] G. B. Ermentrout and J. D. Cowan. "A mathematical theory of visual hallucination patterns". In: *Biological cybernetics* 34.3 (1979), pp. 137–150.

[9] O. Faugeras, R. Veltz, and F. Grimbert. "Persistent neural states: stationary localized activity patterns in nonlinear continuous n-population, q-dimensional neural networks". In: *Neural computation* 21.1 (2009), pp. 147–187.

[10] J. Fraser. "A new visual illusion of direction". In: *British Journal of Psychology* 2.3 (1908), p. 307.

[11] M. A. Giese, G. Schöner, and H. S. Hock. "Neural field dynamics for motion perception". In: *International Conference on Artificial Neural Networks*. Springer. 1996, pp. 335–340.

[12] M. Golubitsky, L. Shiau, and A. Török. "Bifurcation on the Visual Cortex with Weakly Anisotropic Lateral Coupling." In: *SIAM J. Appl. Dyn. Syst.* 2.2 (2003), pp. 97–143.

[13] T. Kato. "Nonlinear semigroups and evolution equations". In: *Journal of the Mathematical Society of Japan* 19.4 (1967), pp. 508–520.

[14] A. Kitaoka, B. Pinna, and G. Brelstaff. "Contrast polarities determine the direction of Café Wall tilts". In: *Perception* 33.1 (2004), pp. 11–20.

[15] H. Klüver. "Mescal and mechanisms of hallucinations". In: *Chicago: University of Chicago* (1966).

[16] I. Leviant. "Does 'brain-power' make Enigma spin?" In: *Proceedings of the Royal Society of London. Series B: Biological Sciences* 263.1373 (1996), pp. 997–1001.

[17] D. M. MacKay. "Moving visual images produced by regular stationary patterns". In: *Nature* 180 (1957), pp. 849–850.

[18] D. M. MacKay. "Visual effects of non-redundant stimulation". In: *Nature* 192.4804 (1961), pp. 739–740.

[19] R. Nicks, A. Cocks, D. Avitabile, A. Johnston, and S. Coombes. "Understanding Sensory Induced Hallucinations: From Neural Fields to Amplitude Equations". In: *SIAM Journal on Applied Dynamical Systems* 20.4 (2021), pp. 1683–1714. eprint: https://doi.org/10.1137/20M1366885.

[20] S. Ôharu. "Note on the representation of semi-groups of non-linear operators". In: *Proceedings of the Japan Academy* 42.10 (1966), pp. 1149–1154.

[21] A. Pazy. *Semigroups of linear operators and applications to partial differential equations*. Vol. 44. Springer Science & Business Media, 2012.

[22] E. L. Schwartz. "Spatial mapping in the primate sensory projection: analytic structure and relevance to perception". In: *Biological cybernetics* 25.4 (1977), pp. 181–194.

[23] S. H. da Silva. "Existence and upper semicontinuity of global attractors for neural network in a bounded domain". In: *Differential Equations and Dynamical Systems* 19.1 (2011), p. 2.

[24] R. Sokoliuk and R. VanRullen. "The Flickering Wheel Illusion: When α Rhythms Make a Static Wheel Flicker". In: *Journal of Neuroscience* 33.33 (2013).

[25] C. Tamekue. "Controllability, visual illusions and perception". PhD thesis. Université Paris-Saclay, Oct. 2023. eprint: https://theses.hal.science/tel-04230895.

[26] C. Tamekue, D. Prandi, and Y. Chitour. "Cortical origins of MacKay-type visual illusions: A case for the non-linearity". In: *IFAC-PapersOnLine* 56.2 (2023). 22nd IFAC World Congress, pp. 476–481. ISSN: 2405-8963.

[27] C. Tamekue, D. Prandi, and Y. Chitour. "Reproducing sensory induced hallucinations via neural fields". In: *2022 IEEE International Conference on Image Processing (ICIP)*. IEEE. 2022, pp. 3326–3330.

[28] P. Tass. "Cortical pattern formation during visual hallucinations". In: *Journal of Biological Physics* 21.3 (1995), pp. 177–210.

[29] R. B. Tootell, M. S. Silverman, E. Switkes, and R. L. De Valois. "Deoxyglucose analysis of retinotopic organization in primate striate cortex". In: *Science* 218.4575 (1982), pp. 902–904.

[30] R. Veltz and O. Faugeras. "Local/global analysis of the stationary solutions of some neural field equations". In: *SIAM Journal on Applied Dynamical Systems* 9.3 (2010), pp. 954–998.

[31] N. Vilenkin. *Special Functions and the Theory of Group Representations*. Trans. by V. Singh. Vol. 22. Translations of Mathematical Monographs. American Mathematical Society, Dec. 1968.

[32] H. R. Wilson and J. D. Cowan. "A mathematical theory of the functional dynamics of cortical and thalamic nervous tissue". In: *Kybernetik* 13.2 (1973), pp. 55–80.

[33] S. Zeki, J. D. Watson, and R. S. Frackowiak. "Going beyond the information given: the relation of illusory visual motion to brain activity". In: *Proceedings of the Royal Society of London. Series B: Biological Sciences* 252.1335 (1993), pp. 215–222.

Université Paris-Saclay, CNRS, CentraleSupélec, Laboratoire des signaux et systèmes, 91190, Gif-sur-Yvette, France
Email address: cyprien.tamekue@centralesupelec.fr

Université Paris-Saclay, CNRS, CentraleSupélec, Laboratoire des signaux et systèmes, 91190, Gif-sur-Yvette, France
Email address: dario.prandi@centralesupelec.fr

Université Paris-Saclay, CNRS, CentraleSupélec, Laboratoire des signaux et systèmes, 91190, Gif-sur-Yvette, France
Email address: yacine.chitour@centralesupelec.fr